Land Use Policy 143 (2024) 107213

Contents lists available at ScienceDirect

Land Use Policy

journal homepage: www.elsevier.com/locate/landusepol

Impact of urban compactness on carbon emission in Chinese cities: From moderating effects of industrial diversity and job-housing imbalances

Xing Xiaoxu [a], Xi Qiangmin [a,*], Shi Weihao [b]

[a] School of Applied Economics, Renmin University of China, No. 59 Zhongguancun Street, Beijing 100872, China
[b] School of Architecture, Tianjin University, No.92, Weijin Road, Tianjin 300072, China

ARTICLE INFO

Keywords:
Urban compactness
Urban form
Carbon emission
Industrial diversity
Job-housing imbalances

ABSTRACT

In the context of sustainable urban space utilization and carbon neutrality, this study systematically explores the relationship between urban form and carbon emissions in China from 2005 to 2020. Utilized night-light and Open-source Data Inventory for Anthropogenic CO_2 data from 260 cities to measure urban form and carbon emissions, the threshold effect of urban form on carbon emissions was identified, and the moderating effects of industrial diversity and job-housing imbalances were explored. The results of the study show that, firstly, as urban form becomes compact, carbon emissions within built-up areas and cities both show a trend of decreasing and then increasing. In small and medium-sized cities, urban compactness tends to reduce carbon emissions, while in large and mega-cities, a more compact urban form increases carbon emissions. In addition, in cities with high industrial diversity and low job-housing imbalances, a more compact urban form helps to reduce carbon emissions. To optimize the carbon reduction benefits of urban compactness, our study offers urban planners' insights for comprehensive planning that integrates urban form with both production and residential considerations.

1. Introduction

Global warming and other climate issues have attracted increasing attention worldwide. Numerous studies have shown that global warming is mainly caused by the emissions of carbon dioxide generated by human activities (IPCC, 2021; Ottelin et al., 2019; Pichler et al., 2017). Cities, as central hubs of human activity and energy use, are leading contributors to carbon emissions (Liu et al., 2022a; Yang et al., 2022). While occupying only 2% of the world's land area, urban-driven carbon emissions are responsible for 75% of global carbon emissions, largely driven by fossil fuel consumption (Shi et al., 2022). With the acceleration of industrialization and urbanization, China has become one of the major emitters of CO_2. At the 75th United Nations General Assembly in 2020, China committed to reaching peak CO_2 emissions by 2030 and striving for carbon neutrality by 2060, known as the dual carbon goal or "Double Carbon" target. Amid the imperative to curtail carbon emissions, cities have emerged as foundational entities in this endeavor. "Urban compactness," geometrically interpreted as "urban form" (Marshall et al., 2019), represents a snapshot of urbanization. It not only signifies the efficiency of resource distribution and spatial deployment in a city (Wang et al., 2015), but also reflects factors such as land use dynamics and building density, which play a critical role in dictating carbon emissions within cities (Cai et al., 2021). To achieve the "Double Carbon" target, a thorough exploration of the mechanisms of how urban compactness influences CO_2 emissions at the city level in China, as well as the moderating effects of urban functions on this, is a key prerequisite for developing a low-carbon development path.

At present, widely acknowledged methods for reducing carbon emissions encompass adjusting energy structure, developing non-fossil fuels, inventing negative emission technologies, establishing low-carbon pilot cities, and creating green markets (Liu et al., 2022b). The relationship between urban form and CO_2 emissions, central to these measures' implementation, has increasingly attracted scholarly focus (Fang et al., 2015; Wang et al., 2019). On one hand, urban planners emphasize the positive role of compact urban form in reducing carbon emissions, particularly from the perspective of minimizing infrastructure-related transportation emissions (Falahatkar and Rezaei, 2020). Correspondingly, urban complexity and fragmentation have been identified as factors contributing to increased carbon emissions through the four domains of land utilization efficiency, built structures, transportation systems, and developmental trends (Hong et al., 2022). On the other hand, ambiguities still linger regarding the impact of urban

* Corresponding author.
E-mail addresses: xingxiaoxu@ruc.edu.cn (X. Xiaoxu), xqm@ruc.edu.cn (X. Qiangmin), whshi666@tju.edu.cn (S. Weihao).

https://doi.org/10.1016/j.landusepol.2024.107213
Received 23 August 2023; Received in revised form 4 March 2024; Accepted 19 May 2024
Available online 30 May 2024
0264-8377/

compactness and urban spatial development patterns on carbon emissions. For instance, research by Shi et al. (2022) has merely illustrated the significance of compact urban form for carbon reduction in some Chinese cities. The increase in concentration and compactness can amplify the urban heat island effect which often leads to higher energy consumption and private vehicle use for cooling purposes (Ding et al., 2022; Ou et al., 2019). The resulting surge in electricity demand, particularly during the summer months, can increase by up to 20% in some regions, thereby elevating carbon emissions (Debbage and Shepherd, 2015). Given these contrasting findings, the quantitative relationship between the degree of urban compactness and carbon emissions, as well as the positive and negative impact mechanisms, remains unclear (Gao et al., 2022). It becomes crucial to investigate as to whether there is a specific point or range at which the benefits of urban compactness are maximized with respect to reducing emissions; our interest is in exploring the possibility of a threshold effect, or even the exhibition of a "U" shaped relationship. A simplistic approach to compact urban form is not a one-size-fits-all solution for carbon emission reduction.

According to research by Gaigné et al. (2012), the distribution of residents and industries within a city may impact the relationship between urban form and carbon emissions. Carbon emissions stemming from urban expansion or the shape of the city are predicated on estimates of energy consumption related to industrial operations and human activities. This establishes that one of the critical factors influencing actual CO_2 emissions is the industrial structure and human behaviors, where the effects of urban form on carbon emissions can easily be influenced by these underlying variables (Zheng et al., 2023). On the industrial level, the industrial structure has become a widely recognized factor affecting carbon emissions. Studies have shown that the intensity of the impact of spatial patterns on carbon emissions varies for cities dominated by different industrial types, with compact urban form being more conducive to carbon reduction in industrial cities (Shi et al., 2020).

On the level of human activity, considering that degree of jobs-housing imbalance significantly affects urban commuting, and therefore influence the transportation carbon emissions. Merely pursuing economic activity and land compactness, without adequately addressing the imbalance between occupational locations and residential areas, may only have a marginal impact on the reduction of carbon emissions (Ewing and Cervero, 2010b). However, most previous research has focused on urban form as a representative factor of urban development (Wang et al., 2015; Wu et al., 2022). Recognizing that urban space merely serves as the "workplaces" for carbon emissions, a comprehensive analysis of the relationship between urban form and carbon emissions requires the incorporation of the influence of industrial structure and urban jobs-housing conditions.

In general, although research has begun to investigate the impact of urban built-up area spatial morphology on carbon emissions across spatial and temporal scales, the use of cross-sectional or city-group-level samples has constrained the understanding of the dynamic, holistic relationship between urban form and carbon emissions (Jung et al., 2022). Furthermore, the majority of the research has concentrated on correlation analysis, failing to uncover the mechanisms by which multi-centered urban forms affect carbon emissions, which includes potential mediating or moderating effects that may be present in this process (Zheng et al., 2023). Consequently, fundamental questions remain unanswered: How does urban form affect carbon emissions, and what factors influence this relationship?

To address these questions, we identified the built-up areas of 260 Chinese cities from 2005 to 2020 based on nighttime light data and uses Open-source Data Inventory for Anthropogenic CO_2 (ODIAC) data for carbon emission measurement. Due to the non-linear relationship between urban spatial patterns and carbon emissions, it is crucial to understand if there is a tipping point or threshold in urban spatial patterns beyond which the impact on carbon emissions changes significantly. We initially investigated the threshold effect of urban spatial patterns on carbon emissions, then considered industrial diversity indices and job-housing imbalances as moderating variables from the industrial and residential perspectives, respectively, to explore their influence on how urban form affects carbon emissions. The potential novel contributions of this research include: (i) Expanding the temporal and spatial dimensions of the study of the relationship between urban form and carbon emissions, exploring the threshold mechanisms affecting carbon emissions. (ii) Clarifying the moderating effects of urban production and residential aspects on how urban compactness influences carbon emissions. (iii) Selecting appropriate instrumental variables to enhance the accuracy of variable relationship identification. (iv) Identifying carbon emissions within the built-up area by the extent of the built-up area, and double data validation with carbon emissions within the whole distinct.

The article is structured as follows: Section 2 presents theoretical hypotheses; Section 3 describes measurement issues and model specification; Section 4 analyzes the basic empirical results; Section 5 conducts further research of moderating effects; Section 6 offers discussion and policy recommendations; Concludes is shown in the Section 7.

2. Theoretical hypotheses

2.1. Impact of urban compactness on carbon emissions

With the aggregation of urban resources and population, the compact city has become a widely accepted model for low-carbon urban construction (Li et al., 2022a). A compact urban form implies higher land use density and concentrated resources, which aligns with the principles of smart growth (Dieleman and Wegener, 2004). Smart growth emphasizes sustainable urban planning by focusing on higher density, mixed-use development, and the preservation of green spaces, thereby promoting both carbon sink protection and energy consumption reduction (Cirilli and Veneri, 2014). However, is a compact urban form invariably associated with decreased carbon emissions? The answer is complex.

Research has identified a nonlinear response and a threshold effect in the relationship between urban carbon emissions and their driving factors (Chen and Zhou, 2021). Scholarly contributions, notably those of Chen et al. (2008) and Liu et al. (2014), posit that the benefits of compact cities in reducing emissions are limited to a certain scope. Beyond this threshold, the advantages may diminish or invert because of dense populations and constrained public service resources (Shi et al., 2022). Evidence suggests that urban compactness increases carbon emissions through factors such as traffic congestion and heat island effects (Ding et al., 2022), which increase carbon emissions through additional transportation fuel and high-temperature cooling (Gössling et al., 2023; Santamouris et al., 2015). However, this relationship varies based on city size, with larger cities experiencing intensified heat island effects and traffic congestion costs due to more complex urban forms (Liu et al., 2021b; Rao et al., 2021). This corroborates research of Ou et al. (2019) that increased compactness in major urban areas may hinder CO_2 reduction in first-tier cities, while decreasing emissions in others.

Theoretically, the threshold in the relationship between urban compactness and carbon emissions can be summarized. Before this threshold, compact urban form brings positive externalities of agglomeration, such as reducing commuting distances, enhancing public transport viability, and lowering infrastructure costs(Wang et al., 2017; Zhao et al., 2010). Moreover, compact cities increase energy efficiency, yielding significant carbon reduction effects (Xia et al., 2019). However, surpassing this threshold may lead to diseconomies of agglomeration, causing issues like heat island effects (Zhou et al., 2017), traffic congestion (Yang et al., 2012), and insufficient green space (Jim and Chan, 2016), thereby potentially offsetting or even boosting carbon emissions. In summary, the spatial form of urban built-up areas has a fluctuating effect on carbon emission intensity, which decreases and then increases. This complex interplay leads us to propose Hypothesis 1, emphasizing that the relationship between compact urban form and carbon emissions is nuanced and subject to various considerations.

Hypothesis 1. : Under a combination of agglomeration economies and agglomeration diseconomies, compact urban form and carbon emissions exhibit a U-shaped correlation.

2.2. The moderating role of urban industrial diversity

The impact of urban form on carbon emissions has emerged as a multifaceted issue. The compact city model, though favored by some, is not a one-size-fits-all solution. Along with increasing urban compactness, strategies influencing the distribution of residents and businesses within and between cities must also be considered (Gaigné et al., 2012). This leads to the question of whether the impact of urban form on CO_2 emissions is modulated by residential living and industrial production.

Urban compactness's impact on carbon emission may differ according to a city's industrial structure. Research demonstrates that urban form complexity significantly impacts CO_2 emissions, with industrial cities experiencing the most pronounced effects, followed by service cities and other urban types (Shi et al., 2020). Furthermore, the industrial structure plays a key role in determining how urban form influences carbon emissions. To elaborate, as industrial firms become more dependent on the import of raw materials and the export of industrialized products, complex urban forms often lead to increased use of freight vehicles (Fan et al., 2018). Furthermore, the intensified carbon emission effects in eastern coastal cities might stem from excessive manufacturing concentration, leading to a "factor congestion effect" (Shi et al., 2022; Su et al., 2014). This constrains technological innovation in enterprises, resulting in diminishing returns to scale and an increase in CO_2 emissions. A moderating effect of industrial structure in the interplay between urbanization and carbon emissions in China has been confirmed (Cheng et al., 2022; Luqman et al., 2023). The observed differences in carbon emission patterns across cities with varying industrial structures highlight the need for urban planning and environmental policies that take into account the specific industrial composition (Zheng et al., 2023). To some extent, industrial diversity can reflect the industrial structure, which encompasses a broader range of economic dynamics than industry structure (Jensen, 2016; Simon, 1987). While industry structure typically examines the composition and dominance of specific sectors, industry diversity captures the variety and balance of multiple sectors coexisting within an urban environment (Beaudry and Schiffauerova, 2009). This comprehensive view is crucial for understanding the complex interactions between various industries and urban form, which in turn affect carbon emissions.

Focusing on industrial diversity, we organize the mechanisms by which it may regulate the reduction of carbon emissions in compact urban forms. First, industrial diversity promotes synergy and resource sharing among different industries, thereby reducing energy consumption and carbon emissions (Bettencourt et al., 2007). A compact urban form further enhances this synergy, enabling more efficient resource use. Secondly, industrial diversity encourages local production and consumption, potentially diminishing the need for long-distance transportation. Within a compact urban structure, shorter commuting distances and more efficient public transit systems further reduce carbon emissions (Cervero and Murakami, 2010). Additionally, industrial diversity bolsters a city's resilience to economic and environmental risks. Compact urban form can facilitate this adaptability by offering more effective resource allocation and planning, thereby making cities more responsive to sustainability challenges (Ramaswami et al., 2018). Finally, industrial diversity can foster cross-industry technological innovation and knowledge sharing. A compact urban form can reinforce these interactions, stimulating cleaner and more efficient methods of production, and hence lowering carbon emissions (Frenken et al., 2007). In summary, industrial diversity and compact urban form collectively function to decrease urban carbon emissions by enhancing resource efficiency, optimizing transportation, fortifying adaptability, and advancing innovative technologies. As industrial diversity can enhance pathways to reduce carbon emissions in compact urban forms, we propose Hypothesis 2.

Hypothesis 2. : Industrial diversity reinforces the carbon emission reduction caused by compact urban form.

2.3. The moderating role of urban job-housing imbalances

The imbalance between employment and housing within urban areas can act as a regulator in terms of how compact urban form affects carbon emissions. In areas where employment and housing are relatively unbalanced, residents' demand for public infrastructure is higher, travel distances are longer, and the socio-economic scale is larger. Overcrowding, increased competitive costs, traffic congestion, and excessive demand for infrastructure and operational maintenance may diminish the role of compact urban forms in reducing carbon emissions (Huang and Yuquan, 2019). Building on this, Wang and Chai (2009) advocate for the establishment of a broader framework that encompasses not only urban compactness but also considers the balance between employment and housing, aiming to holistically create more sustainable low-carbon cities.

The relationship between compact urban form and carbon emissions is complicated by job-housing imbalances. This dual impact of imbalances not only undermines the potential of compact urban forms to facilitate public transport use and diminish carbon emissions but also hampers the efficient deployment of multifunctional land use and infrastructure. Job-housing imbalances, characterized by a spatial mismatch between residential areas and employment centers, lead to increased commuting distances (Durst, 2021). Such scenarios often fall outside the purview of efficient public transport networks, compelling residents to rely more on personal vehicles (Zhao et al., 2011), thereby significantly increasing carbon emissions, counteracting the environmental benefits typically associated with compact urban form. Additionally, job-housing imbalances in compact cities frequently culminate in enduring inefficiencies in land utilization and the transportation network. This imbalance necessitates more comprehensive transport land planning and an expansion of the transportation infrastructure (Xiao et al., 2021), directly undermining the carbon emission reductions typically associated with compact urban configurations.

The carbon emission reduction potential of compact urban forms depends heavily on achieving a balance between job locations and housing (Yang et al., 2022). While compact urban forms are designed to enhance infrastructure utilization and promote sustainable transportation modes like public transit and biking (Bibri et al., 2020), the misalignment between residential areas and employment centers can undermine the intended emission reductions of compact urban planning. Conversely, in less compact urban environments, job-housing imbalances also exacerbate the pathways leading to increased carbon emissions associated with less compact urban forms. Effective urban planning must consider this balance to harness the full benefits of compact urban design. Failing to address these imbalances could lead to suboptimal outcomes in which the compactness of the urban form does not translate into the anticipated environmental benefits. Therefore, we propose Hypothesis 3.

Hypothesis 3. : Job-housing imbalances weaken carbon emission reduction caused by compact urban form.

3. Measurement issues and model specification

3.1. Measurement issues

Since compact urban form impacts carbon emissions through two distinct mechanisms: one that decreases emissions (when urban form is compact) and another that increases carbon emissions (when the urban form is over-compact), the relationship presents a certain threshold utility (Hypothesis 1). On this basis, we believe that industrial diversity will allow compact urban form to reduce carbon emissions more prominently, thus strengthening or enhancing the emission reduction benefits of compact urban form (Hypothesis 2). Occupational or residential imbalances also cause the path of compact urban form to reduce carbon emissions more unobtrusively, and thus weaken or diminish the emission reduction benefits of compact urban form (Hypothesis 3). To validate the aforementioned hypotheses, this section delineates the construction of key variables—urban form, urban carbon emissions, industrial diversity, and jobs-housing imbalance—along with instrumental and control variables. The identification of urban form, urban carbon emissions, and instrumental variables employs multidimensional remote sensing data to enhance the readability of the description. The process and framework for constructing the relevant variables are illustrated in Fig. 1.

3.1.1. Description of urban compactness

Compact urban development strategically molds the economic spatial architecture of cities, simultaneously bolstering both development and sustainability. Historically, the measures of urban compactness and density relied on the ratio of built-up areas to total area and population density (Boyko and Cooper, 2011). With the advent of high-precision data, notably through remote sensing, a city's spatial attributes have become pivotal in assessing compactness over density. To achieve new geometric interpretations and indicators for urban compactness, an indicator system primarily revolves around three urban form dimensions (Bibri et al., 2020), with a topological emphasis on nodes (Liu and Tian, 2022) and connections (Baruah et al., 2021), shape-related elements concerning size and regularity (Boarnet et al., 2017), and dynamic attributes linked with growth and structural evolution (Miguel et al., 2016).

In terms of urban form variables, there exists an incompatibility between the two commonly used nighttime light remote sensing datasets, DMSP-OLS and NPP-VIIRS. This discrepancy limits the temporal span of usable nighttime light data series. To overcome this, our study adopts a cross-sensor nighttime light data correction approach based on self-encoders. We utilized a global "NPP-VIIRS-like" nighttime light dataset with a 500-meter resolution and a city-scale accuracy with an R^2 of 0.95, spanning from 2005 to 2020 (Chen et al., 2021).[1] This dataset facilitates the quantification of the overall urban form and characteristics emanating from the perspective of urban expansion. Given the superiority of the threshold extraction method, based on auxiliary data comparison, in meeting the needs of long-time series evolution of urban cluster spatial morphology, our data processing methodology includes steps of calibrating the annual nighttime light data interception thresholds using the built-up area of Beijing (Yang et al., 2020). From this, we derive the built-up area raster of each prefecture-level city from the nighttime light raster using the threshold extraction method (Fig. 1 (a)). Consistent with existing research, a patch was defined as an urban patch if urban and built-up land occupied most of the 1-km × 1-km area (Liu et al., 2012; Rao et al., 2021). Further, for a comprehensive understanding of urban compactness relative to geographic entities, we engaged with morphology-based indicators of urban structure by the Fragstats 4.2 software, particularly: near-circularity index (*Circle*), cohesion index of patches (*Cohesion*), and neighborhood agglomeration index (*Continuity*) (Angel et al., 2020).

$$Circle = \frac{A_j}{A_{circle\ j}} * \frac{A_j}{\sum_{j=1}^{n} A_j}, \tag{1a}$$

$$Cohesion = [1 - \frac{\sum_{j=1}{}^{n} P_j}{\sum_{j=1}{}^{n} P_j \sqrt{A_j}}][1 - \frac{1}{\sqrt{n}}]^{-1}, \tag{1b}$$

$$Continuity = \frac{M_{real\ j}}{M_{access\ j}}. \tag{1c}$$

Circle is expressed as the ratio of area-weighted patch area to the area of its largest outer circle and measures the degree of regularity of urban form. *Cohesion* increases with the proportion of agglomeration patches in the overall sample and reflects the differentiated state of aggregation and dispersion of the urban form from the perspective of intra-plate compactness. *Continuity* is expressed as the ratio of actual neighboring patches to potential maximum neighboring patches, reflecting how integrated or fragmented the urban patches are. Additionally, the potential maximum neighboring patches refer to maximum number of like adjacencies (joins) between pixels of patch type (class) based on the single-count method (Appendix A). In the Equations (1), A_j represents the area of patch j, $A_{circle\ j}$ is the area of the smallest outer circle, P_j is the perimeter of the patch, n is the overall number of patches in the city, $M_{real\ j}$ is the number of real neighboring patches of patch j, and $M_{access\ j}$ is the number of neighboring patches accessible to patch j. More details on urban compactness can be found in Appendix A.

3.1.2. Description of carbon emission

According to the nomenclature proposed by the World Resources Institute/World Business Council for Sustainable Development (WRI/WBSCD), "Scope 1 Emissions" pertain to emissions produced within city limits (Kennedy et al., 2010). Specifically, these emissions arise from sources such as: combustion of fossil fuels, waste processing, industrial activities and product utilization, along with contributions from agriculture, forestry, and other sectors, with fossil fuels being the most numerous (Hachaichi and Baouni, 2021). However, the information provided through the city-level greenhouse gas emission inventories is often discontinuous, varies in scope, and is sometimes even inconsistent (Mia et al., 2019). Furthermore, many cities' greenhouse gas emission inventories are often derived from the confines of administrative delineations that delineate these areas, which rarely correspond with the city's socio-economic realities and functional relationships.

As discussed above, according to research of Van der Borght and Pallares Barbera (2023), we used area of urban built-up area identified in the previous section and the ODIAC, overlayed these two grids, and calculated the total carbon emissions within the built-up area of the city (*Build-Carbon*). And using the ODIAC data, we also accounted for total carbon emissions within the administrative area (*City-Carbon*) (Wiedmann et al., 2010), which can be compared with carbon emissions within the built-up area (Fig. 1(c)).

3.1.3. Description of moderating variables

From the production side and the consumption perspectives, we analyzed the urban form's influence on carbon emissions across various cities. In the production side, we mainly focused on the industrial diversity. Industrial diversity refers to the distribution of economic activity across different industries within a region or country. A diverse industrial base is often associated with economic stability and industrial space layout (Duranton and Puga, 2000). The measurement of industrial diversity has evolved over time, and a variety of indices and methods have been proposed, like the Entropy Index, Ogive Index, National Averages Index, diversity indices based on portfolio theory, CS-Index, and others. Early studies often relied on the Herfindahl-Hirschman Index (HHI) as a measure of diversity (Hannah and Kay, 1977). While primarily used to assess market concentration, it was adapted to gauge industrial diversification. A lower HHI value indicates greater diversity.

[1] The original 'NPP-VIIRS-like' nighttime light dataset is sourced from Chen et.al (2021). For further details, one can refer to the Harvard University Dataverse repository, accessible at "https://dataverse.harvard.edu/dataset.xhtml?persistentId=doi:10.7910/DVN/ YGIVCD", where the associated attachments are available for download.

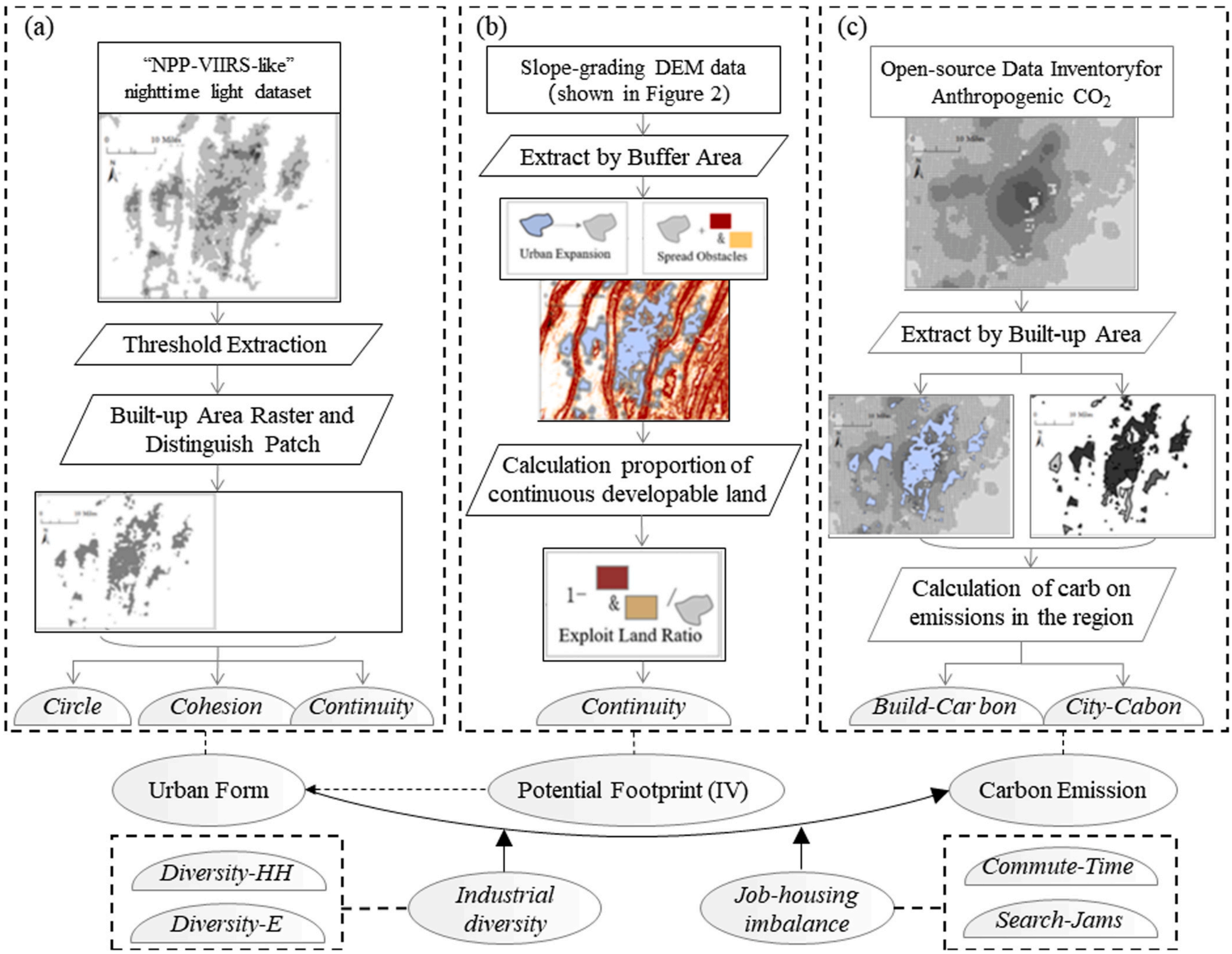

Fig. 1. Variable and theoretical construction framework. Note: To better highlight the process of constructing instrumental variables, the schematic diagram selected Chongqing, a city with complex terrain in China, as the case for the remote sensing data calculation process. The geomorphological landscape of the Chongqing area is complex and diverse, encompassing mountains, hills, plains, and rivers. Among these, mountains account for 81.2% of Chongqing's total area.

Introduced by Shannon (1948), the Entropy Index is also a prominent measure of diversity. It evaluates the proportions of various industrial sectors in the total economy, with higher entropy values denoting greater diversity (Johnston, 1969). Therefore, this paper primarily uses the value of 1 minus the Herfindahl-Hirschman Index to create the industrial diversity index $Diversity - HH_{it}$ to measure industrial diversity. The larger this index, the higher the industrial diversity. Additionally, the Entropy Index, denoted as $Diversity - E_{it}$, is used to measure industrial diversity and is utilized for robustness checks. In the Eqs. (2a) and (2b), $emp_{d,i,t}$ represents the number of people employed in industry d in city i in year t, $emp_{i,t}$ represents the total number of people employed in all industries in city i in year t, represents the proportion of people employed in industry d in city i in year t relative to the total employment in the city.

$$Diversity - HH_{it} = 1 - \sum_{d=1}^{D} \left(\frac{emp_{d,i,t}}{emp_{i,t}} \right)^2 \tag{2a}$$

$$Diversity - E_{it} = \sum_{d=1}^{D} \left(S_{d,i,t} \ln \frac{1}{S_{d,i,t}} \right),\ S_{d,i,t} = \frac{emp_{d,i,t}}{emp_{i,t}} \tag{2b}$$

In the living side, we are primarily interested in the moderating role of job-housing imbalances on urban form and carbon emissions. The urban job-housing imbalances is a phenomenon that describes the imbalance between places to live and places to work within cities. Its commonly used measures include the Jobs-Housing Ratio (JHR) (Cervero, 1989) and the Jobs-Housing Spatial Mismatch Index(Kain, 1968), which analyzes the imbalance between the quantitative structure and spatial distribution of jobs and housing units in a given area or region. For the spatial imbalances of jobs and housing, we used the average urban commuting time divided by the built-up area in prefecture-level cities. Data for commuting time is sourced from the China Family Tracking Survey (CFPS) (Zhao et al., 2011). By dividing this commuting time by the built-up area, we aim to control for city size, thus allowing for a more accurate comparison across different urban areas (Ewing and Cervero, 2010a). To further capture the spatial dynamics of the job-housing imbalance, we utilized the Baidu Index for "traffic jam" and "traffic congestion" keywords, normalized by the resident population. This index, derived from search engine data, serves as a proxy for traffic congestion levels and, importantly, reflects the residents' subjective perceptions and awareness of traffic congestion issues in their city. The utilization of this index as a measure is based on the premise that increased search frequency for these terms indicates a higher level of public concern or experience of traffic-related issues, thereby providing insights into the intensity of the job-housing imbalance from the perspective of city dwellers (Zuiderwijk et al., 2021).

3.1.4. Endogeneity and instrumental variables

The link between urban form and carbon emissions raises concerns of endogeneity, arising primarily from omitted variables and reverse causality. Given similar conditions, cities with enhanced governmental capabilities are more likely to have superior urban planning, stricter sprawl boundaries, and thus, a compact form. Moreover, cities endowed with strong institutional structures and efficient local governance are often more adept at mitigating carbon emissions. While the metric of public service expenditure per unproductive land unit can help account for the influence of local government promotion incentives, there remains an unresolved issue with omitted variables (Yu et al., 2020). Additionally, the possibility of reverse causality, where cities with lower carbon emissions may influence their urban form, complicates the direction of causality (Croci et al., 2017; Xia et al., 2017). To address these issues, we propose the use of instrumental variables that are correlated with urban form but exogenous to carbon emissions. Supplemented by the inclusion of relevant control variables and rigorous sensitivity analyses, the instrumental variable is designed to mitigate the effects of potential endogeneity, thereby ensuring a more robust and accurate understanding of the relationship between urban form and carbon emissions.

We incorporated cities' "Potential Footprint" as an instrumental variable exclusive to the urban form, which remains unrelated to other confounding factors in the regression, allowing for precise coefficient estimations. The "Potential Footprint" is defined as the proportion of continuous developable land areas observed during the urban sprawl process, essentially being the ratio of the largest continuously developable land area to the entire area within a specified radius of urban activity (i.e., buffer zone), whose calculation process includes the following steps. Initially, drawing from the China Natural Resources Office Document No. 127, we pinpointed areas unsuitable for urban construction. As illustrated in Fig. 2, this identification involved a slope-grading procedure using Digital Elevation Model (DEM) data from the Geospatial Data Cloud, followed by adjustments for elevation and terrain variations. After that, utilizing built-up area raster from nighttime lighting data, we evaluated the ratio of the developable area to the entire buffer zone, using a 500-m buffer (*Ratio05*). Additionally, for exogeneity verification, the ratio within a 300-m buffer (*Ratio03*) is employed. These buffer radii derive from historical patterns of urban expansion (Angel et al., 2005; Liu et al., 2021a). Fig. 1(b) illustrates the demarcation boundaries of this instrumental variable, using a segment of Chongqing as a representative example. This variable, fluctuating annually at the city level, acknowledges the diverse topographical challenges cities face throughout their evolution.

"Potential Footprint" metric derives from the exogenous urban extension vector within the buffer zone, as opposed to the observed actual urban sprawl trajectory. Theoretically, *Ratio05* and *Ratio03* are not correlated with the error terms of the other explanatory variables, but with the urban form. Specifically, neither *Ratio05* nor *Ratio03* have a direct bearing on enterprise production, residential living dynamics and local governance efficiency, aligning with the exogeneity criteria (Mariaflavia, 2020). Crucially, cities demonstrate varying sprawl rates across developable versus non-developable terrains. When the buffer zone contains more developable land, it leads to a symmetrical outward expansion of urban areas. This symmetric expansion enhances the connectivity between urban blocks, ensuring closer integration of urban blocks and efficient spatial organization, thereby fostering urban compactness (Peng et al., 2020). Hence, the primary influence of *Ratio03* and *Ratio05* on carbon emissions stems from their impact on urban spatial configurations and agglomerative traits, meeting the correlation criteria.

3.1.5. Control variables

For the control variables we mainly considered GDP per capita, built-up area, public service expenditure per unit of unproductive land, population, fixed asset investment/gross domestic product, and percentage of high carbon emitting enterprises(Heinonen et al., 2020; Sun et al., 2022). The sources of the control variables were also the China Urban Statistical Yearbook, the China Urban Construction Statistical Yearbook, and the EPS database. After variable matching, linear

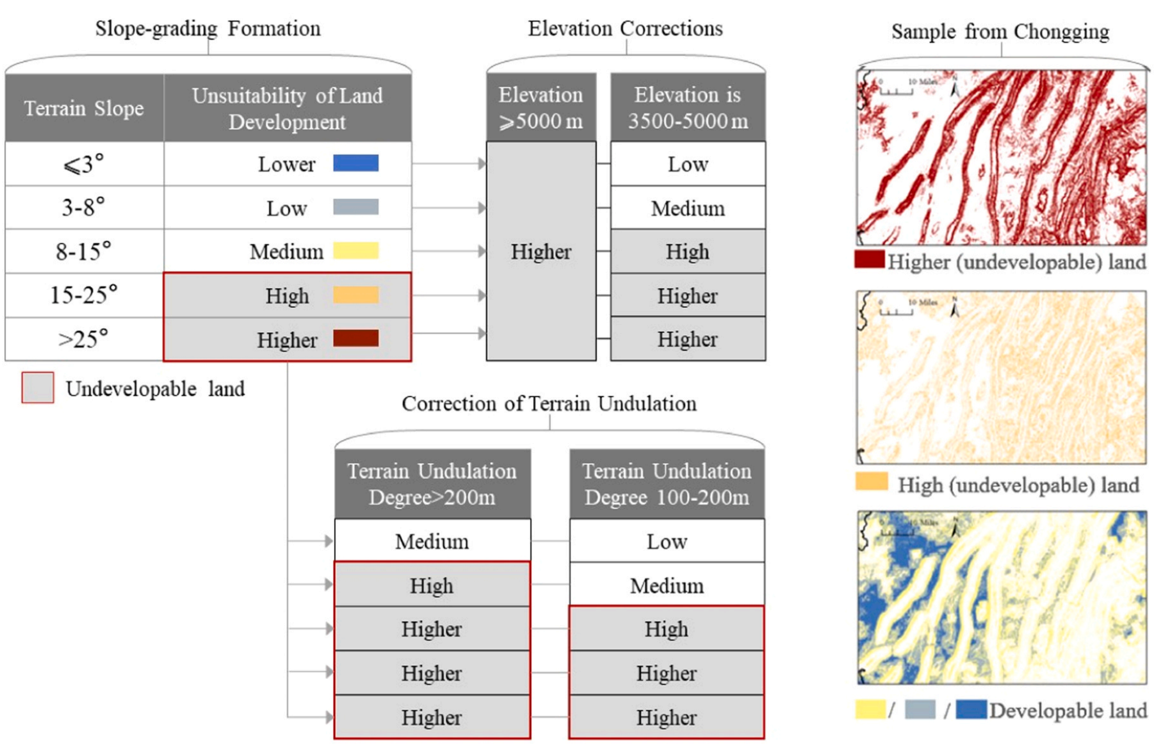

Fig. 2. Slope-grading procedure in instrument variable recognition path. Note: The categories "Lower," "Low," and "Medium" (cool colors) represent areas more suitable for development, and categories "High" and "Higher" (warm colors) indicate undevelopable areas.

interpolation of missing values, and extreme value processing, the total sample size was fixed at 4,160 samples from 260 cities in 2005–2020. Summary statistics for the main variables are shown in Table 1. The time evolution trend chart of explanatory variables is shown in Fig. 3 and the spatiotemporal evolution trend of the variables can be found in Appendix B.

3.2. Model specification

Following the theoretical analysis and the provided hypotheses, the subsequent models have been established.

(i) Nonlinear relationship of urban form on carbon emission

$$Carbon_{it} = \alpha_0 + \alpha_1 Shape_{it} + I(K \leq Shape_{it})\alpha_2(Shape_{it} - K) + \beta_1 Control_{it} + \varepsilon_i + \delta_t + \mu_{it}, \tag{3}$$

In the nonlinear regression model of urban form affecting carbon emission (Eq. (3)), $Carbon_{it}$ represents the carbon emissions within built-up areas ($Build - Carbon_{it}$) and city administrative areas ($City - Carbon_{it}$). On the right side, as shown in the above equation, $Shape_{it}$ is the urban form index, and we measured urban form in three ways as $Circle_{it}$, $Continuity_{it}$ and $Cohesion_{it}$. K is the threshold value that when $Shape_{it}$ is less than K, the regression coefficient for $Shape_{it}$ is α_1, and when $Shape_{it}$ is less than K, the regression coefficient is $\alpha_1 + \alpha_2$ (Seo et al., 2019). Further, to ensure internal validity of models, city-level control variables $Control_{it}$, city fixed effect ε_i and time fixed effect δ_t were controlled. And μ_{it} is the residual term of each city at time t, where i is a sample of 260 cities after data treatment, and t represents the 2005–2020 period.

(ii) Further discussion of the nonlinear relationship of urban form on carbon emission

$$Carbon_{it} = \alpha_0 + \alpha_1 Shape_{it} + \alpha_2 Shape_{it}^{\ 2} + \beta_1 Control_{it} + \varepsilon_i + \delta_t + \mu_{it}, \tag{4a}$$

$$Carbon_{it} = \alpha_0 + \alpha_1 Shape_{it} Group_j + \beta_1 Control_{it} + \varepsilon_i + \delta_t + \mu_{it}, \tag{4b}$$

In Eqs. (4a) and (4b), the model extends the nonlinear regression framework of urban form's impact on carbon emissions to accommodate the influence of city group membership. For Eq. (4a), the model includes both a linear term ($Shape_{it}$) and a quadratic term ($Shape_{it}^{\ 2}$) for the urban form index. The inclusion of the quadratic term allows for the exploration of nonlinear relationships between urban form and carbon emissions. Eq. (4b) is designed to capture the differential effects of urban form across various city groups on carbon emissions, where $Group_j$ represents the group membership variable and j ranges from 1 to 4, presenting small cities, medium cities, large cities, and megacities. Furthermore, small cities are those with a stable urban populace under 500,000; medium cities have a population ranging from 500,000–1 million; large cities encompass those with 1–5 million inhabitants; and megacities are characterized by an urban population exceeding 5 million (National Development [2014] No. 51).

(iii) Regression model of the moderating effects on industrial diversity

$$Carbon_{it} = \lambda_0 + \lambda_1 * Shape_{it} + \lambda_2 Shape_{it} Producing_{it} + \lambda_3 Producing_{it} + \beta_1 Control_{it} + \varepsilon_i + \delta_t + \mu_{it}, . \tag{5}$$

(iv) Regression model of the moderating effects on jobs-housing imbalance

$$Carbon_{it} = \rho_0 + \rho_1 * Shape_{it} + \rho_2 Shape_{it} Living_{it} + \rho_3 Living_{it} + \beta_1 Control_{it} + \varepsilon_i + \delta_t + \mu_{it}, \tag{6}$$

In the regression model of the moderating effects, $Producing_{it}$ is the industrial diversity index and $Living_{it}$ is the jobs-housing imbalance index which are moderating variables of the relationship between urban form and carbon emission. $Producing_{it}$ is measured from both industry

Table 1
Descriptive statistics.

Variable	Name	Definition	Source	Mean	S.D	Min	Max
Dependent Variable	*Build-Carbon*	Carbon emissions within built-up areas	ODIAC	0.43	0.76	0.01	3.38
Carbon[a]	*City-Carbon*	Carbon emissions within cities		26.17	16.26	3.98	72.65
Instrumental Variable	*Ratio03*	Developable area/total area in the 300 m buffer	NPP-VIIRS-like' nighttime light & DEM dataset	0.91	0.11	0.57	1.00
Ratio	*Ratio05*	Developable area/total area in a 500 m buffer		0.93	0.11	0.57	1.00
Explanatory Variables	*Circle*	Near-circularity index	NPP-VIIRS-like' nighttime light dataset	0.65	0.20	0.00	1.00
	Continuity	Proximity agglomeration index		0.60	0.21	0.00	1.00
Shape	*Cohesion*	Cohesion index of patches		0.84	0.20	0.00	1.00
Moderating Variables	*Diversity-HH*	Industry Herfindahl-Hirschman Index	EPS database	0.83	0.06	0.63	0.90
Industrial diversity	*Diversity-E*	Entropy index of industrial employment ratio		2.23	0.22	1.62	2.56
Job-housing imbalance	*Commute-Time*	Average urban commuting time / built-up area	CFPS	0.28	0.26	0.02	1.99
	Search-Jams	Baidu Index for "traffic jam" and "traffic congestion" keywords / resident population	Baidu Index	1.55	2.76	0.00	25.22
Control Variables	*Agdp*	GDP per capita	The China Urban Statistical Yearbook, the China	3.80	2.79	0.59	11.74
	Area	Built-up area	Urban Construction Statistical Yearbook and the EPS	117.76	127.84	20.00	615.71
	Govfis	Public service expenditure per unit of unproductive land	database.	0.14	0.04	0.01	0.26
	People	Logarithmic number of the resident population		5.88	0.62	4.57	6.98
	Invest	Regional fixed asset investment/GDP		0.66	0.28	0.24	1.34
	Carbonind[b]	Percentage of high carbon emitting enterprises		0.43	0.34	0.04	1.00

[a] The carbon emission raster for 2020 is obtained from the trend raster projection and adjusted to the 2020 data from China Carbon Accounting Databases (CEADs).

[b] The selection criteria for high carbon-emitting industries were established in accordance with the "National Carbon Emission Trading Covered Industry and Code" and the "Benchmark and Baseline Levels of Energy Efficiency in Key High-Energy-Consuming Industries." Data were derived from the Chinese Industrial Enterprise Database spanning the years 2005–2013. For subsequent years, the proportion of the secondary industry was used to perform linear regression interpolation, ensuring continuity and accuracy.

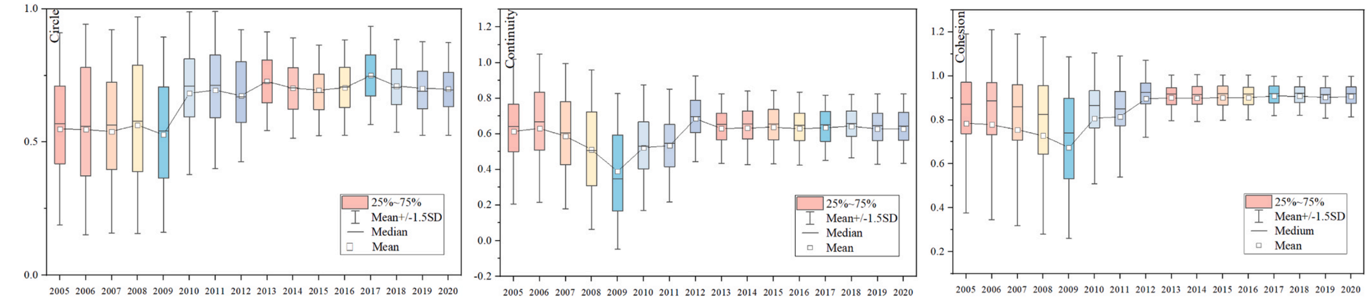

Fig. 3. Time evolution trend chart of explanatory variables *Shape*.

Herfindahl-Hirschman methods ($Diversity - HH_{it}$) and Entropy methods ($Diversity - E_{it}$). $Living_{it}$ is measured from both commuting time per built-up area ($Commute - Time_{it}$) and the Baidu Index for "traffic jam" and "traffic congestion" keywords per resident population ($Search - Jams_{it}$). In this study, we utilized the Two-Stage Least Squares (2SLS) instrumental variable model to address the issue of endogeneity. In the first stage, the instrumental variable $Ratio_{it}$ is used to estimate the part of the potentially $Shape_{it}$ variable that is uncorrelated with the error term, which means in IV regress model $Shape_{it}$ in Eqs. (3) to (6) are estimated by Eq. (7). For the basic nonlinear relationship of urban form on carbon emission, we used $Ratio03_{it}$ in the main regression and $Ratio05_{it}$ in the robustness check. For further discussion of this nonlinear relationship, the instrumental variables for *Shape* and $Shape^2$ are *Ratio03, Ratio05* and $Ratio03^2$, $Ratio05^2$. For moderating effects on industrial diversity and jobs-housing imbalance, the instrumental variables for *Shape* and *Shape # Producing* are *Ratio03, Ratio05* and *Ratio03# Producing, Ratio05# Producing* and the instrumental variables for *Shape* and *Shape # Living* are *Ratio03, Ratio05* and *Ratio03# Living, Ratio05# Living*.

$$Shape_{it} = \omega_0 + \omega_1 Ratio_{it} + \beta_1 Control_{it} + \varepsilon_i + \delta_t + \mu_{it}, \tag{7}$$

The framework of the empirical evidence of our study is presented as follows Fig. 4.

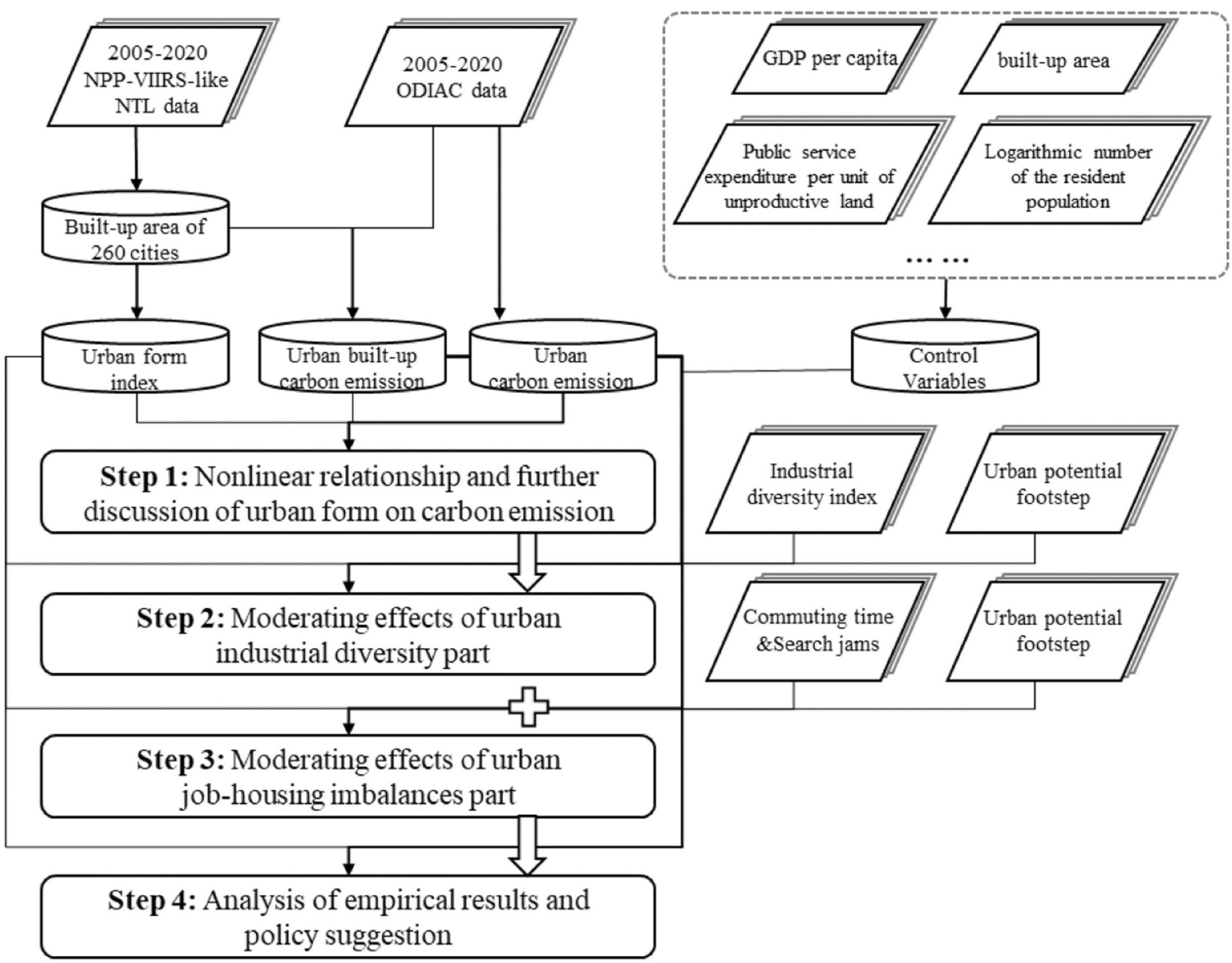

Fig. 4. The technology roadmap for research.

4. Analysis of basic empirical results

4.1. Threshold regression results of urban compactness on carbon emissions

Table 2 presents the threshold model regressions results considering potential footprint *Ratio* as the instrumental variable and columns (1)–(3) show the threshold model regression results of urban form on carbon emissions within built-up areas based on 2005–2020 indices. Per the results of a one-stage regression of these instrumental variables, coefficients in the one-stage regression of urban form and potential footprint indicators were significant at the 1% level, passing exogeneity and weak identification tests, thereby satisfying the exogeneity and correlation requirements (Acemoglu et al., 2001; DellaVigna and Kaplan, 2007; Meng et al., 2023) (Appendix C). From the preliminary model's regression results, as *Shape-b* is related to the α_1 in the Eq. (3), the results indicate that urban morphological variables ("*Circle*", "*Continuity*", "*Cohesion*") in all models have a significant negative correlation with carbon emissions. For example, the coefficient for the "*Circle*" variable in Table 2 (2) is -0.841, indicating that at the start, the more compact the urban shape is, the less carbon it may emit. Similarly, *Continuity* and *Cohesion* are also negatively correlated with carbon emissions, which may suggest that a more continuous and tighter urban fabric may be associated with lower carbon emissions. However, "Kink_slope" in represents α_2 in the Eq. (3), which means that when the compactness of the urban form is higher than the threshold value, the coefficient of its impact on carbon emissions is $\alpha_1 + \alpha_2$. For instance, when *Circle* is less than 0.486, the coefficient for the "*Circle*" variable in column (1) is -0.841, but when *Circle* is more than 0.486, the coefficient for the "*Circle*" variable in column (1) is 0.769. The same conclusion still holds in the relationship between *Continuity* and *Cohesion* with carbon emissions within built-up areas. The regression result of this threshold effect makes the relationship between spatial form of compact cities and carbon emissions show a first decreasing and then increasing trends.

Table 2 columns (4)–(6) show the threshold model regression results of urban form on carbon emissions within cities based on administrative scale. The impact of urban form on carbon emissions within built-up areas (e.g., those in residential, commercial, and industrial areas) and within administrative districts (e.g., at the citywide or county/regional scale) may differ. In terms of spatial extent, built-up areas are usually concerned with finer urban spatial scales, and administrative areas usually cover a wider geographical area, including urban, suburban and rural areas. In terms of influencing factors, carbon emissions from built-up areas are likely to be more influenced by building design, transportation patterns and land use. Carbon emissions from administrative areas may involve a wider range of factors, including industrial production, energy supply and waste management. A comparison of the results from the columns (1)–(3) and columns (4)–(6) shows that the basic variable relationships remain consistent. That is, there is also a first decrease and then an increase in the impact of compact urban form on carbon emissions within cities. However, in columns (4)–(6), firstly, because of the volume of urban carbon emissions, the compact urban form has a greater coefficient of influence on urban carbon emissions. Secondly, the possible explanation we give for the much smaller threshold for the effect of urban form compactness on urban built-up areas is that administrative areas may include suburban and rural areas of the city, which may be more dependent on private vehicles. Thus, even smaller increases in compactness may rapidly lead to increased traffic congestion and carbon emissions.

4.2. Robustness testing

To enhance the underlying assumptions, robustness tests were conducted as described below.

(i) Replacing the dependent variable: In Table 3, we used the sum of carbon emissions from Scope 1 and Scope 2 for city areas as a proxy for carbon emissions (*Carbon-Scope*) (Pichler et al., 2017). Scope 1 refers to all direct emissions within urban areas, including greenhouse gas emissions from transportation and buildings, industrial processes, agriculture, forestry and land-use change, and waste disposal activities. Scope 2 refers to indirect energy-related emissions occurring outside urban areas, including emissions from purchased electricity, heating and/or cooling for urban consumption.

(ii) Replacing explanatory variable: In the pursuit of enhancing

Table 2
Regression results of urban form on carbon emissions within built-up areas.

DV: *Carbon*	*Build-Carbon*			*City-Carbon*		
EV: *Shape*	(1) *Circle*	(2) *Continuity*	(3) *Cohesion*	(4) *Circle*	(5) *Continuity*	(6) *Cohesion*
Shape-b	-0.841***	-0.561***	-0.356***	-26.718***	-29.237***	-28.917***
	(-27.457)	(-10.286)	(-16.764)	(-3.900)	(-27.827)	(-17.576)
Agdp	0.011***	0.013***	0.025***	-0.447***	0.408***	0.800***
	(9.294)	(11.166)	(17.539)	(-11.973)	(8.695)	(15.437)
Area	0.001***	0.000***	0.001***	-0.044***	-0.015***	0.007***
	(29.662)	(8.836)	(21.493)	(-31.307)	(-7.534)	(4.595)
Govfis	1.359***	-1.917***	-0.724***	80.435***	-68.970***	-44.563***
	(10.039)	(-15.784)	(-5.630)	(15.088)	(-11.941)	(-8.611)
People	0.162***	1.476***	0.667***	79.929***	52.565***	-14.626***
	(4.875)	(51.684)	(9.507)	(29.900)	(25.162)	(-9.458)
Invest	0.095***	0.209***	0.143***	13.739***	11.188***	15.361***
	(11.967)	(24.332)	(11.594)	(42.713)	(42.061)	(41.237)
Carbonind	-0.007***	-0.002***	-0.006***	-0.613***	-0.321***	-0.404***
	(-37.025)	(-11.172)	(-19.837)	(-43.482)	(-24.202)	(-41.666)
Kink_slope	1.610***	0.751***	3.084***	15.484**	93.738***	85.317***
	(23.494)	(16.285)	(24.859)	(2.292)	(39.223)	(35.577)
Threshold value	0.486***	0.654***	0.919***	0.120***	0.651***	0.788***
	(38.588)	(23.236)	(365.829)	(3.874)	(401.923)	(98.177)
Year	YES	YES	YES	YES	YES	YES
City	YES	YES	YES	YES	YES	YES
Observations	4,160	4,160	4,160	4,160	4,160	4,160

Notes: DV and EV are short for dependent variable and explanatory variable. Threshold value is the threshold *K* in Eq. (3). *Shape-b* is the coefficient when the urban form indicators (*Circle, Continuity, Cohesion*) are less than the threshold *K*. *Kink_slope* is the additional coefficient when the urban form indicators (*Circle, Continuity, Cohesion*) are more than the threshold *K*. The instrumental variable is *Ratio05*, and tables of threshold regression are the same. The t-value under the cluster robust standard error is in parentheses; The instrumental variables are Ratio05; *, **, *** indicate significant at the significance level of 10%, 5%, and 1%, respectively. The tables below are the same.

Table 3
Regression Results of urban form on carbon emissions (Replacing dependent variable).

DV: *Carbon-Scope*; EV: *Shape*	(1) *Circle*	(2) *Continuity*	(3) *Cohesion*
Shape-b	-0.170***	-0.095***	-0.399***
	(-21.329)	(-16.121)	(-23.990)
Kink_slope	0.224***	0.186***	0.538***
	(23.657)	(33.530)	(39.516)
Threshold value	0.341***	0.625***	0.854***
	(29.642)	(83.034)	(164.674)
Year	YES	YES	YES
City	YES	YES	YES
Observations	4,160	4,160	4,160

robustness, a substitution approach was employed for urban form explanatory variables (Table 4). Firstly, the landscape shape index (Eq. 7a) was utilized as a proxy variable to quantify *Circle* patterns, devoid of area weighting. Notably, when the landscape comprises a solitary circular patch, the *Lsi* equals 0. The value of the near-circularity index experiences a decline when the shape of patches within the landscape deviates from regular circular patterns or displays irregularities.

In a parallel vein, *Diver* and *Polo* were harnessed as substitute metrics for gauging *Cohesion* and *Continuity*. These metrics serve to delineate the extent of urban polycentricity and the degree of inter-center aggregation, both derived from LandScan remote sensing data. *Diver* is precisely defined in Eq. 7b, whereinP_{centre} denotes the population residing in each subcenter within the city, while P_{total} signifies the cumulative population of all population centers. This measure encapsulates the relative significance of subcenters in comparison to the primary center. A larger *Diver* index value denotes an increased prominence of subcenters and a greater uniformity in the concentration of each center within the city.

Furthermore, *Polo* is formulated as presented in Eq. 7c, where m represents the number of identified centers, d_k signifies the distance from center k to other centers, and x_k denotes the population of center k. Elevating values of the *Polo* indicator correlate with improved connectivity among various centers, suggesting enhanced interconnectivity within the urban landscape.

$$Lsi = 1 - P_k \Big/ 2\sqrt{\pi S_k}, \tag{7a}$$

$$Diver = \frac{P_{centre}}{P_{total}} \tag{7b}$$

$$Polo = \sqrt{\sum_{k=1}^{m} \frac{(I_k - \overline{I})^2}{m}} \Bigg/ \left(\frac{I_{\max}}{2}\right); I_k = x_k * d_k; I_{\max} = x_{\max} * d_{k\ max} \tag{7c}$$

Table 5 presents the robustness test results for substituting instrumental variables and the sample interval, taking the explanatory variable *Circle* as an example. The robustness test results with explanatory variables *Continuity* and *Cohesion* can be found in Appendix D. (iii) In Table 5 columns (1)–(2), we made a strategic switch in our approach by introducing the "*Ratio03*", which represents the proportion of developable land to the total land within a 300 m buffer, serving as the instrumental variable for urban form. (iv) To ensure a more robust testing process, in Table 5 columns (3)–(4), we've adjusted our approach by excluding data from the 2007–2008 period, which was marked by the financial crisis. (v) For a more comprehensive understanding, in Table 5 columns (5)–(6), we adjusted our dataset by excluding provincial capital cities. This approach was taken to assess the stability and consistency of our findings. Gratifyingly, the outcomes align seamlessly with the primary conclusions presented earlier in the main content.

4.3. *Further discussion of urban compactness on carbon emissions*

The regression results in Table 6 provide insights into the relationship between urban form and carbon emissions that instrumental variable models consistently highlight a U-shaped relationship. Specifically, as cities adopt an initially more circular urban form, there's a discernible reduction in carbon emissions, as indicated by the negative coefficient for the *Shape* variable. Yet, as compactness of urban form continues to grow, this benefit starts to wane and reverses, leading to increased carbon emissions, which the positive coefficient for $Shape^2$ captures. While Table 6 explores a continuous, nonlinear U-shaped relationship, Table 2 emphasizes the existence of distinct regimes or phases in the relationship, demarcated by the threshold values. Both approaches are complementary, offering a comprehensive view of how urban form factors influence carbon emission outcomes, but through different conceptual lenses—one through a smooth curvature and the other through distinct phases separated by thresholds. Further reinforcing the validity of this analysis, the relevant tests, support the appropriateness and strength of the chosen instrumental variable. In sum, these results robustly attest to the nuanced role urban form plays in influencing carbon emissions, underscoring the initial benefits of compactness of urban form which, beyond a certain threshold, begin to diminish, which means the following table presents U-shaped relationship of urban form on carbon emissions, corresponding to Table 2 in the previous section.

Table 7 explores the association between urban form and carbon emissions in cities of different scales. Within the *Build-Carbon* perspective (columns (1)–(4)), a pronounced negative link between urban form and carbon emissions is observed in small cities, indicated by a coefficient of -2.351 at a significance level below 0.01. This negative trend persists, albeit less significantly, in medium cities. Transitioning to the *City-Carbon* perspective, the results showcase no significant trend in small cities (columns (5)–(6)). However, medium cities depict a noteworthy negative relationship, with large and mega-cities exhibiting significant positive coefficients (columns (7)–(8)). Seemingly unrelated regression (SUR) highlights the differences in regression coefficients across groups. This finding suggests that in areas where the urban form is not compact enough, such as small and medium-sized cities, increased compactness leads to positive agglomeration externalities and reduced carbon emissions. In areas with relatively high urban compactness, such as large and mega-cities, the agglomeration diseconomies of a compact urban form begin to dominate, leading to an increase in urban carbon emissions.

Table 4
Regression results of urban form on carbon emissions (Replacing explanatory variable).

DV: *Carbon*	*Build-Carbon*			*City-Carbon*		
EV: *Shape*	(1) *Lsi*	(2) *Diver*	(3) *Polo*	(4) *Lsi*	(5) *Diver*	(6) *Polo*
Shape-b	-2.165***	-1.661***	-0.533***	-113.786***	-143.747***	-54.270***
	(-34.113)	(-42.576)	(-3.376)	(-19.279)	(-12.422)	(-41.911)
Kink_slope	2.415***	1.986***	1.354***	97.548***	173.423***	45.672***
	(34.535)	(38.181)	(7.759)	(16.494)	(14.234)	(24.186)
Threshold value	0.237***	0.603***	0.598***	0.100***	0.536***	0.588***
	(61.756)	(68.675)	(72.792)	(35.136)	(188.921)	(44.752)
Year	YES	YES	YES	YES	YES	YES
City	YES	YES	YES	YES	YES	YES
Observations	4,160	4,160	4,160	4,160	4,160	4,160

Table 5
Regression results of urban form on carbon emissions (Replacing IV and sample).

DV: *Carbon*	Replacing IV		Replacing Time		Replacing Cities	
EV: *Circle*	(1) *Build-Carbon*	(2) *City-Carbon*	(3) *Build-Carbon*	(4) *City-Carbon*	(5) *Build-Carbon*	(6) *City-Carbon*
Shape-b	-1.191***	-11.549***	-0.397***	-9.345***	-0.714***	-1.765**
	(-14.849)	(-10.114)	(-12.211)	(-9.890)	(-40.874)	(-2.540)
Kink_slope	1.595***	86.193***	0.638***	48.634***	1.121***	81.435***
	(17.983)	(40.522)	(15.053)	(26.012)	(20.618)	(18.245)
Threshold value	0.528***	0.662***	0.582***	0.694***	0.699***	0.807***
	(78.543)	(228.759)	(46.373)	(161.969)	(98.443)	(123.175)
Observations	4,160	4,160	3,640	3,640	3,776	3,776
Year	YES	YES	YES	YES	YES	YES
City	YES	YES	YES	YES	YES	YES

Table 6
U-shaped relationship regression results of urban form on carbon emissions.

DV: *Carbon*	*Build-Carbon*			*City-Carbon*		
EV: *Shape*	(1) *Circle*	(2) *Continuity*	(3) *Cohesion*	(4) *Circle*	(5) *Continuity*	(6) *Cohesion*
Shape	-2.460*	-0.099	7.263*	-42.705*	-75.758***	240.642***
	(-1.945)	(-0.101)	(1.907)	(-1.794)	(-3.085)	(2.699)
Shape^2	1.935*	0.098	-5.645**	25.069*	68.602***	-170.230***
	(1.906)	(0.112)	(-1.996)	(1.995)	(3.096)	(-2.690)
Observations	4,160	4,160	4,160	4,160	4,160	4,160
UI test	29.72***	31.08***	89.85***	29.72***	31.08***	89.85***
WI test	16.24***	10.98***	21.93***	16.24***	10.98***	21.93***
OI test	7.96**	10.77***	10.32***	16.28***	14.99***	22.32***
Year	YES	YES	YES	YES	YES	YES
City	YES	YES	YES	YES	YES	YES

Notes: The instrumental variables for *Shape* and *Shape*^{2} are *Ratio03, Ratio05* and *Ratio03*^{2}*, Ratio05*^{2}. The unidentifiable test (UI test) is the result of the Kleibergen–Paap rk LM statistic. The weak instrumental variable test (WI test) is the result of the Cragg–Donald Wald F statistic and the overidentification test of all instruments (OI test) is the result of the Hansen J statistic. The tables below are the same.

Table 7
Relationship regression results of urban form on carbon emissions at different stages of cities.

DV: *Carbon*	*Build-Carbon*				*City-Carbon*			
EV: *Circle*	(1) Small-cities	(2) Medium-cities	(3) Large-cities	(4) Mega-cities	(5) Small-cities	(6) Medium-cities	(7) Large-cities	(8) Mega-cities
Circle	-2.351***	-0.331**	0.016	0.025	-1.018	-33.237*	68.576**	104.459**
	(-3.433)	(-2.404)	(0.167)	(0.353)	(-0.256)	(-1.772)	(2.354)	(2.030)
SUR	7.69*				6.34*			
UI test	88.93***	10.89**	11.73**	15.44***	88.93***	10.89**	11.73**	15.44***
WI test	39.88***	3.631*	4.265**	9.34*	39.88***	3.63*	4.27**	9.34*
OI test	7.43**	2.62	5.07**	5.82**	18.37***	2.56	4.99**	5.80**
Observations	1,656	1,279	937	288	1,656	1,279	937	288
Year	YES	YES	YES	YES	YES	YES	YES	YES
City	YES	YES	YES	YES	YES	YES	YES	YES

5. Analysis of moderating effects

5.1. Moderating effects of industrial diversity

Table 8 analyzes the moderating effects of industrial diversity (*Producing)*, denoted as "*Diversity-HH*" and "*Diversity-E*", on the influence of urban form (*Circle, Continuity, Cohesion*) on carbon emissions within built-up areas (*Build-Carbon*). Columns (1)–(3) illustrate the moderation effect under the framework of the Herfindahl-Hirschman Index for industrial diversity, whereas columns (4)–(6) portray the moderating effect according to the entropy index framework. In an attempt to control for endogeneity issues related to industrial diversity and urban form, instrumental variables have been employed throughout. In Eq. (5), the interaction term "*Shape # Producing*" serves as a moderator. This interaction term is negative and significant across all (1)–(6) columns, indicating that an increase in industrial diversity attenuates the path through which urban compactness enhances carbon emissions. Concurrently, this implies that as industrial diversity rises, the path through which urban compactness reduces carbon emissions is amplified. This amplification may be attributable to the enhanced interplay among different industries, culminating in a more efficient allocation of resources and utilization of energy, hence diminishing carbon emissions. Such efficiency may be accentuated within compact urban structures, where logistics, transportation, and communication are typically more streamlined (Duranton and Puga, 2004).

Table 9 introduces a new dimension to our understanding by replacing the explanatory variables with carbon emissions within cities. The table highlights the intriguing interplay of industrial diversity on the connection between compact urban form and carbon emissions. As indicated by Table 9, when examining the relationship of compact urban form to built-up area carbon emissions, industrial diversity's moderating impact seems more pronounced than its effect on the urban carbon emissions within cities. It may because industrial diversity tends to have a more direct interaction with compact urban spatial form within built-up areas (Bettencourt et al., 2007). The synergies between different industrial sectors might be more pronounced within the confines of the

Table 8
Regression results for moderating effects of industrial diversity on carbon within built-up areas.

DV: *Build-Carbon*	*Diversity-HH*			*Diversity-E*		
MV: *Producing*						
EV: *Shape*	(1) *Circle*	(2) *Continuity*	(3) *Cohesion*	(4) *Circle*	(5) *Continuity*	(6) *Cohesion*
Shape	1.424**	1.272***	1.112***	1.269**	1.145***	1.037***
	(2.185)	(2.800)	(2.770)	(1.968)	(2.869)	(2.650)
Producing	0.057**	0.043*	0.054**	0.062***	0.050**	0.059**
	(2.458)	(1.762)	(2.354)	(2.638)	(2.017)	(2.544)
Shape # Producing	-0.965**	-1.085**	-0.660*	-0.348***	-0.379**	-0.248**
	(-2.216)	(-2.271)	(-1.935)	(-2.626)	(-2.560)	(-2.370)
UI test	16.41***	114.01***	50.72***	15.48***	112.20***	49.41***
WI test	7.82**	36.11***	17.38***	8.66**	37.71***	16.86***
OI test	1.06	10.04***	6.30**	1.73	10.59***	4.60*
Observations	4,160	4,160	4,160	4,160	4,160	4,160
Year	YES	YES	YES	YES	YES	YES
City	YES	YES	YES	YES	YES	YES

Notes: DV, MV and EV are short for dependent variable, moderating variable and explanatory variable. The variables in the model are standardized. The explanatory and moderating variables are centered. The instrumental variables for *Shape* and *Shape # Producing* are *Ratio03*, *Ratio05* and *Ratio03# Producing*, *Ratio05# Producing*. The tables below are the same.

Table 9
Regression results for moderating effects of industrial diversity on carbon within cities.

DV: *City-Carbon*	*Diversity-HH*			*Diversity-E*		
MV: *Producing*						
EV: *Shape*	(1) *Circle*	(2) *Continuity*	(3) *Cohesion*	(4) *Circle*	(5) *Continuity*	(6) *Cohesion*
Shape	2.511***	0.652	1.511***	2.292***	0.253	1.361***
	(3.406)	(1.584)	(3.844)	(3.063)	(0.720)	(3.509)
Producing	-0.141	-0.534	-0.002	0.023	-0.062	0.048
	(-0.333)	(-1.303)	(-0.006)	(0.190)	(-0.514)	(0.544)
Shape # Producing	-0.036	-0.055**	-0.047**	-0.039*	-0.054**	-0.049**
	(-1.586)	(-2.557)	(-2.253)	(-1.683)	(-2.501)	(-2.361)
UI test	16.41***	114.01***	50.72***	15.48***	112.20***	49.41***
WI test	7.82**	36.11***	17.38***	8.66**	37.71***	16.86***
OI test	1.767	22.35***	12.02***	2.859	22.01***	11.76***
Observations	4,160	4,160	4,160	4,160	4,160	4,160
Year	YES	YES	YES	YES	YES	YES
City	YES	YES	YES	YES	YES	YES

built-up region, leading to more efficient energy use and transportation, thereby reducing carbon emissions.

5.2. Moderating effects of the job-housing imbalance

Table 10 analyzes the moderating effects of the job-housing imbalance (*Living)*, denoted as "*Commute-Time*" and "*Search-Jams*", on the influence of urban compactness (*Circle, Continuity, Cohesion*) on carbon emissions within built-up areas (*Build-Carbon*). Columns (1)–(3) illustrate the moderating effect under structural imbalance between jobs and housing as measured by average commuting time per build-up area, whereas columns (4)–(6) portray the moderating effect according to the spatial imbalance between jobs and housing as measured by the Baidu Index for "traffic jam" and "traffic congestion" keywords per resident population. In Eq. (6), the interaction term "*Shape # Living*" serves as a moderator. This interaction term is positive across all (1)–(6) columns, indicating that the job-housing imbalance exacerbates the impact of urban compactness on carbon emissions within built-up areas.

Table 10
Regression results for moderating effects of job-housing imbalance on carbon within built-up areas.

DV: *Build-Carbon*	*Commute-Time*			*Search-Jams*		
MV: *Living*						
EV: *Shape*	(1) *Circle*	(2) *Continuity*	(3) *Cohesion*	(4) *Circle*	(5) *Continuity*	(6) *Cohesion*
Shape	-0.342*	-0.306	-0.202	-0.071	-0.026	-0.097
	(-1.839)	(-1.303)	(-1.056)	(-0.446)	(-0.139)	(-0.386)
Living	0.012	-0.013	-0.030	0.097	0.205	0.105
	(0.307)	(-0.335)	(-0.655)	(0.526)	(0.700)	(0.380)
Shape # Living	0.051**	0.083*	0.058*	0.196*	0.340	0.289*
	(1.978)	(1.729)	(1.650)	(1.700)	(1.464)	(1.695)
UI test	30.46***	22.38***	20.09***	58.40***	29.16***	12.82***
WI test	14.29***	7.23**	6.42**	22.54***	7.69**	9.38***
OI test	5.60*	4.06*	11.14***	5.75*	3.94	7.19**
Observations	654	654	654	3,120	3,120	3,120
Year	YES	YES	YES	YES	YES	YES
City	YES	YES	YES	YES	YES	YES

Notes: The instrumental variables for Shape and *Shape # Living* are Ratio03, Ratio05 and Ratio03# *Living*, Ratio05# *Living*. The tables below are the same.

Consistent with the hypothesis analysis, the importance of urban compactness in reducing carbon emissions decrease when the job-housing imbalance increases. In other words, when the compactness of the urban form is certain, the job-housing imbalance increases carbon emissions. Concurrently, this implies that as the job-housing imbalance rises, the path through which urban compactness reduces carbon emissions is amplified.

This result can be attributed to several underlying factors. For example, the job-housing imbalance may lead to an increased demand for transportation, transport options changes, and an inefficient use of urban land and infrastructure. Firstly, in compact urban areas, the increased job-housing imbalance can strain the transportation network. Despite shorter potential commuting distances, the mismatch between job locations and housing can lead to longer commutes, particularly if employment centers are heavily concentrated in certain areas while housing is located elsewhere. This spatial mismatch undermines the carbon emission reductions typically associated with compact urban structures. Secondly, compact urban environments, while typically more efficient in public transportation, might not fully counteract the effects of the job-housing imbalance. If the public transportation network is not adequately aligned with the actual flow of commuters, or if capacity is insufficient during peak hours, residents might still opt for private vehicles. This reliance on personal transportation can offset the potential emission reductions from compact urban form. Additionally, while compact urban form encourages mixed land use, a significant job-housing imbalance can disrupt the balance. For instance, if housing areas are not adequately integrated with job centers, the benefits of having residential, commercial, and recreational spaces in close proximity are diminished, which leads to higher carbon emissions. In essence, while urban compactness has its inherent advantages in reducing carbon emissions, the effectiveness of urban compactness in lowering carbon emissions depends heavily on the harmonious integration of residential and employment areas.

The findings presented in Table 11 explore the moderating effects of the job-housing imbalance on the association between compact urban form and urban carbon emissions. Furthermore, they exhibit congruence with those observed when considering carbon emissions within built-up areas as the dependent variable. In urban planning and carbon emissions analysis, the job-housing imbalance appears to have a statistically significant influence when examining the interplay between compact urban form and emissions from built-up areas. In contrast, its role seems less pronounced when we consider the broader relationship between compact urban form and the carbon emissions within built-up areas. Citywide analyses encompass a more diverse range of land use and activities, capturing the cumulative effects of spatial mismatches and inefficiencies in urban planning, which may not be apparent in built-up areas. Consequently, the broader urban canvas provides a more comprehensive understanding of the relationship between compact urban form, job-housing imbalance, and carbon emissions, underscoring the critical need for holistic urban planning strategies that address these dynamics on a larger scale.

6. Discussion

6.1. Discussion on the relationship between variables

Our findings have confirmed a nuanced interplay between compact urban form and carbon emissions. This U-shaped distribution implies that up to a certain threshold, compact cities yield tangible carbon reduction effects. However, beyond this threshold, the adverse effects such as heat island phenomena, traffic congestion, and diminished green spaces come into play. Consistency with existing research (Ding et al., 2022; Hong et al., 2022; Sun et al., 2022), this highlights the need for optimal urban density that ensures reduced emissions without overstretching urban capacities. This breaking point in urban compactness thus becomes a vital indicator for sustainable urban planning.

Industrial diversity's moderating role on the relationship between urban form and carbon emissions provides fascinating insights into how different economic activities can influence environmental outcomes. Mechanistically, cities with diverse industries benefit from synergistic operations, reduced energy consumption, and lesser reliance on long-distance transportation—all of which reduce carbon emissions. Compact urban forms further amplify these effects by enhancing local production and consumption dynamics and promoting efficient transportation modes. Furthermore, although a compact urban form can effectively reduce carbon emissions by shortening commuting distances and improving the efficiency of public transportation (Jin et al., 2022), a high imbalance between working and housing leads to longer commuting distances and higher traffic congestion, thereby diminishing the benefits of urban compactness and increasing carbon emissions.

Our analysis on carbon emissions explores the thresholds of urban density, the influence of industrial diversity, and the impact of job-housing imbalances, highlighting the complexity of sustainable urban development. The identification of these thresholds is crucial and lays the groundwork for future research in urban planning that incorporates sustainability into urban design. This research encourages further investigation into how urban density can be optimized for environmental benefits without adverse effects. Additionally, our examination of how industrial diversity influences urban carbon emissions underscores the importance of integrating urban planning with economic structuring for sustainability. Our findings also contribute to the evidence that sustainable urban mobility and a balance between jobs and housing are essential, especially as cities approach a critical level of compactness. This emphasizes the need for research on sustainable urban mobility and mixed land use to reduce carbon emissions, mitigating the negative impacts of compact urban form. Given our findings'

Table 11
Regression results for moderating effects of job-housing imbalance on carbon within cities.

DV: *City-Carbon*	*Commute-Time*			*Search-Jams*		
MV: *Living*						
EV: *Shape*	(1) *Circle*	(2) *Continuity*	(3) *Cohesion*	(4) *Circle*	(5) *Continuity*	(6) *Cohesion*
Shape	-0.455**	-0.412*	-0.332	-0.182	-0.257	-0.220
	(-2.473)	(-1.777)	(-1.613)	(-1.317)	(-1.320)	(-1.034)
Living	-0.098**	-0.119***	-0.172***	0.335**	0.870***	0.393*
	(-2.134)	(-2.827)	(-3.380)	(2.204)	(2.850)	(1.655)
Shape # Living	0.142***	0.172***	0.135***	0.339**	0.971***	0.568**
	(2.870)	(2.777)	(2.831)	(2.108)	(2.916)	(1.992)
UI test	30.46***	22.38***	20.09***	58.40***	29.16***	12.82***
WI test	14.29***	7.23**	6.42**	22.54***	7.69**	9.38***
OI test	9.637***	5.93*	7.322**	12.96***	5.15*	15.65***
Observations	654	654	654	3,120	3,120	3,120
Year	YES	YES	YES	YES	YES	YES
City	YES	YES	YES	YES	YES	YES

implications for urban planning, environmental sustainability, and economic development, we call for an interdisciplinary approach to study the interplay between urban form, industrial diversity, job-housing imbalances, and carbon emission.

6.2. Policy and practice recommendations for urban planning

Based on the provided hypotheses and their implications, we can focus on specific policy and practice recommendations for urban planning. Firstly, urban planning should enhance compact urban development strategically. However, considering the U-shaped relationship between urban compactness and carbon emissions, a nuanced approach to compact urban development is necessary. For medium-sized cities, pursuing urban compactness more aggressively can maximize emission reduction benefits. Meanwhile, in large cities like Beijing and Shanghai, careful evaluation is required to ensure that the degree of compactness does not surpass a threshold where it starts to have adverse effects, such as heat island phenomena and traffic congestion.

Secondly, fostering industrial diversity and improving transportation should be considered. Industrial diversity can enhance the pathways of urban compactness in reducing carbon emissions, promoting diverse industrial development, and encouraging cross-sector collaboration can leverage synergy among different sectors, reducing energy consumption and emissions. This can be complemented by incentivizing local production within compact urban structures, reducing the need for long-distance transportation. In regions characterized by a significant imbalance between job locations and housing, the integration of residential and employment planning is crucial to fully harness the carbon emission reduction potential inherent in urban compactness. Moreover, urban planning must balance the needs for housing affordability and sustainable low-carbon development. This includes investing in green infrastructure and incorporating more green spaces, ensuring that compactness benefits are not offset by socio-economic disparities.

Additionally, different city types and regions require specific attention. Industrial cities, for example, should cater planning to their particular industrial needs and potentials for carbon reduction. Coastal cities need careful planning to avoid excessive manufacturing concentration, which could constrain technological innovation and increase emissions. By understanding these complex relationships between urban form, industrial diversity, job-housing imbalance, and carbon emissions, tailored strategies can be developed.

6.3. Contributions and limitations

In contrast to studies focusing on specific cities and regions in China (Cai et al., 2023; Zhang et al., 2023), our research significantly expands the temporal and spatial dimensions of the study of the relationship between urban form and carbon emissions by exploring the threshold mechanisms across 260 Chinese cities from 2005 to 2020. Moreover, based on remote sensing data, we have identified carbon emissions separately at the city level and at the built-up area level. As research into the optimal urban form from an environmental perspective progressively deepens (Sun et al., 2022; Zheng et al., 2022), we further clarified the threshold effects and U-shaped relationships on how urban form influences carbon emissions. Compared to traditional correlation analysis and panel regression (Lan et al., 2023), through the use of ODIAC data and the selection of appropriate instrumental variables, this study enhances the accuracy of variable relationship identification. Additionally, although existing studies have combined economic factors and urban form as influencing factors of carbon emissions (Li et al., 2022b), there is still a lack of discussion of the complex mechanisms that influence it (Zhu and Hu, 2023). This study further discusses the moderating effects of urban form on carbon emissions in the context of both industrial diversity and job-housing imbalance adjustments.

While this study brings fresh perspectives and contributions to the table, it is not without its limitations. Primarily focusing on Chinese urban settings potentially narrows the generalizability of our findings to other global metropolitan areas whose urbanization features are not very pronounced. Additionally, although we incorporated several novel moderating variables, there might be other pivotal elements that have not yet been explored. In particular, we did not fully consider the ecological and environmental factors of cities, which could impact the levels of carbon emissions and other variables, thereby affecting the relationships among these variables. Moreover, we utilized Beijing as a benchmark for calibrating the built-up area data as reported in the yearbook. While this approach has been validated within reasonable error margins in data and literature (Feng et al., 2020; Jiuwen et al., 2024), it does not comprehensively account for the distinct internal heterogeneity of each of the 260 cities examined. Future research could benefit from exploring a more nuanced methodology in threshold determination, one that acknowledges and integrates the unique characteristics inherent to each city. Future studies should also delve deeper into individual attributes and behavioral tendencies, as these can shape urban form and carbon emissions. Regarding industry diversity and the jobs-housing imbalance, more precise measurement methods could be employed. Delving into micro-level data through means such as surveys, in-depth interviews, and field investigations might enhance the richness and accuracy of our insights. In sum, while we've made strides in shedding light on these areas, there are ample avenues for further research and nuanced understanding.

7. Conclusion

This investigation sheds light on the nuanced interrelationship between urban compactness and carbon footprints in Chinese metropolises. A distinct U-shaped trajectory reveals the benefits and challenges tied to urban density. At the outset, condensed urban settings experience advantages from shorter commutes and streamlined transportation, leading to fewer emissions. However, once surpassing a certain density threshold, drawbacks such as urban heat islands and heightened congestion emerge, hinting at the need for a balanced urban density approach.

Delving deeper, we highlight the pivotal role of industrial diversity in bolstering environmental benefits associated with compact city structures. Such diversity fosters collaborative endeavors across sectors, curtails energy usage, and diminishes reliance on far-reaching transportation—collectively contributing to lowered carbon emissions. Alongside this, the pronounced influence of the jobs-housing disparity on emissions accentuates the call for comprehensive urban planning that marries physical form with socio-economic considerations. From a pragmatic standpoint, the importance of adopting a thoughtful approach to compact urbanization is evident. Tailoring interventions to the distinct attributes of cities can help avoid the challenges linked to extreme compactness. Promoting a mosaic of industries and refining transportation systems, especially in regions grappling with significant jobs-housing imbalances, can amplify the prospects for carbon reduction.

While our study offers invaluable insights into the multifaceted dynamics of urban structure, industrial variety, and carbon release, its primary emphasis on Chinese settings denotes certain boundary conditions. Nonetheless, these revelations provide a springboard for global cities to recalibrate their urbanization paradigms in pursuit of a more sustainable and flourishing future. Going forward, the academic canvas should expand to cover untouched factors, individual predispositions, and more granular data capture methodologies to further enrich this domain.

Funding

The National Natural Science Foundation of China (Grant No. 72003190).

Declaration of Competing Interest

none.

Data availability

Data will be made available on request.

Appendix A. Urban compactness indicators' specific definitions

In our manuscript, we delve into the intricate relationship between urban form and its consequent impact on carbon emissions by employing a set of refined landscape metrics to quantitatively capture the essence of urban morphology. Derived from the robust analytical framework of Fragstats 4.2, these metrics—*Circle, Cohesion, and Continuity*—serve as pivotal variables in our study. The specific descriptions of the indicators are as follows, with the spatial schematic representation of the indicators illustrated in Table A-1.

Circle: This metric quantifies the circularity of a patch by comparing its area to that of the smallest circumscribing circle encompassing it. The Circle index, ranging from 0 to 1, approaches unity for patches nearing circular perfection and dwindles towards zero for more elongated forms. This index, as conceptualized by Fragstats 4.2 Related Circumscribing Circle Index, remains unaffected by the size of the patch, offering an objective measure of shape irrespective of spatial scale. Of note is the fact that due to the constraints of grid data, achieving an index value of exactly one is implausible, underscoring the inherent limitations of digital representations of natural forms.

Cohesion: The index assesses the degree of connectivity or the physical cohesion of patches within a landscape. It is calculated by inversely relating the sum of patch perimeters to the aggregate perimeter adjusted by patch area, normalized against the landscape's cell count. This index encapsulates the landscape's collective connectivity, with values nearing one indicating a highly interconnected mosaic of patches. Fragstats 4.2 Patch Cohesion Index notes that this index is particularly sensitive to the spatial aggregation of patches, enhancing as patches coalesce, thereby reflecting the landscape's cohesive structure.

Continuity: The Adjacency Aggregation Index in Fragstats 4.2, named *Continuity*, evaluates the compactness of patch distribution by comparing the actual to the potential maximum like adjacencies. A simplified explanation of "the potential maximum neighboring patches refer to maximum number of like adjacencies (joins) between pixels of patch type (class) based on the single-count method" is as follows:

(i) When we talk about adjacencies, we are referring to instances where two pixels (or cells) are directly next to each other on a map.

(ii) Single-count method means that when tallying adjacent pixel pairs, each pair is counted only once. This method ensures no double-counting during the tally.

(iii) Maximum Number of Like Adjacencies refers to the maximum number of adjacent pairs that pixels of a specific land cover class can form across all possible spatial arrangements. This maximum is calculated assuming that all pixels of that class are clustered together in the most compact shape possible. In other words, if all pixels are gathered into a single, compact mass, they would form the maximum number of adjacencies.

(iv) According to the definition, the maximum number of adjacencies depends on the area of class i (in number of pixels) and the most compact arrangement those pixels could form. If Ai is the area of class i (in pixels), n is the side length of the largest integer square smaller than Ai, and m is the remainder after subtracting n squared from Ai, then the maximum number of adjacencies can take one of three forms, depending on the value of m: When m=0, it means that class i can perfectly form an n×n square, and the maximum number of adjacencies is 2 n(n-1); When m=n, it means that in addition to a complete n×n square, there's an extra row or column of n pixels, making the maximum number of adjacencies 2 n(n-1) + 2 m – 1; When m>n, it means that beyond a complete n×n square, there's an extra row or column with more than n pixels, so the maximum number of adjacencies is 2 n(n-1) + 2 m - 2.

Expressed as a percentage, *Continuity* offers insights into the spatial arrangement of patches, with values escalating as patches amalgamate into a singular, cohesive entity. This metric, intricately designed to count each like adjacency singularly, disregards landscape boundaries to focus purely on internal patch dynamics, thereby providing a distilled measure of landscape aggregation. More specific details of the metrics can be found in the official documentation of Fragstats 4.2 software.

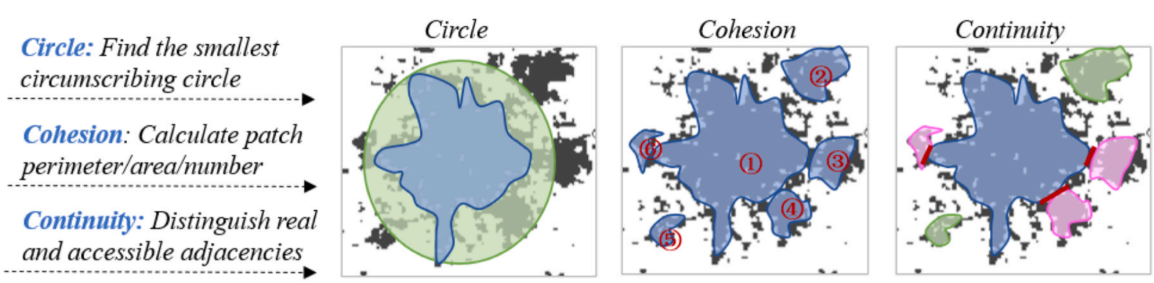

Fig. A1. Schematic definition of urban form variable using Beijing in 2020 as an example.

Appendix B. The spatiotemporal evolution trend of the variables

Carbon emissions are increasingly concentrated in central cities of urban agglomerations, and from 2010 to 2020, the overall carbon emissions showed a declining trend. In terms of morphological indicators, '*Circle*' does not show a clear regional trend, while '*Cohesion*' and '*Continuity*' exhibit a more compact geographical distribution in the eastern coastal areas. Furthermore, the regional descriptive statistics from 2005 to 2020 reveal that, except for the western region, other areas show a pattern evolution from compactness to dispersion. For the industrial diversity index, the most notable change is the significant decline in the diversity of industries in the Northeast region over the decade. Regarding the job-housing imbalance index, the concentration of '*Commute-Time*' in the central and western regions is mainly due to the larger built-up area in the eastern coastal regions, while '*Search-Jams*', reflecting subjective traffic congestion, are mainly concentrated in the eastern regions and have worsened over time.

Appendix C. Tests for instrument variables

The following table presents the regression results when the instrumental variables are *Ratio03* and *Ratio05*; both are considered instrumental variables. From the results in Table C1, it can be seen that instrumental variables statistically significantly affect the endogenous variables and are considered to satisfy the correlation condition.

Table C1
Instrument variable one-stage regression results on carbon.

DV: *Shape*	IV: *Ratio03*			IV: *Ratio05*		
EV: *Ratio*	(1) *Circle*	(2) *Cohesion*	(3) *Continuity*	(4) *Circle*	(5) *Cohesion*	(6) *Continuity*
Ratio	0.070*	0.398***	0.315***	0.199***	0.444***	0.230***
	(1.827)	(9.321)	(7.414)	(5.558)	(11.041)	(5.938)
F-test	13.90***	36.35***	65.06***	13.90***	36.35***	65.06***
Observations	4,160	4,160	4,160	4,160	4,160	4,160
Control	YES	YES	YES	YES	YES	YES
Year/Province	YES	YES	YES	YES	YES	YES

Notes: The t-value under the cluster robust standard error is in parentheses; The instrumental variables are Ratio05; *, **, *** indicate significant at the significance level of 10%, 5%, and 1%, respectively. The tables below are the same.

Table C2 presents the results of exogeneity tests for the instrumental variables *Ratio03* and *Ratio05* in a model examining the relationship between *Shape* (*Circle*, *Cohesion*, *Continuity*) and *Carbon*. The Sargan-Hansen test and the Basmann test were conducted to assess the validity of the instrumental variables. The results of these tests are presented along with their corresponding P-values (in parentheses). For the Sargan-Hansen test, the statistics range from 0.214 to 2.613, with P-values varying between 0.106 and 0.643. Similarly, for the Basmann test, the statistics range from 0.212 to 2.475, with P-values between 0.116 and 0.645. These P-values, being generally above the conventional threshold of 0.05, suggest that the instrumental variables are valid and do not violate the exogeneity restrictions.

Table C2
Tests of overidentification for instrument variable (*Ratio03 & Ratio05*).

DV: *Carbon*	*Build-Carbon*			*City-Carbon*		
EV: *Shape*	(1) *Circle*	(2) *Cohesion*	(3) *Continuity*	(4) *Circle*	(5) *Cohesion*	(6) *Continuity*
Sargan-Hansen test	1.194	0.214	0.996	1.6153	0.996	2.613
	(0.274)	(0.643)	(0.318)	(0.204)	(0.318)	(0.106)
Basmann test	1.180	0.212	0.984	1.596	0.984	2.475
	(0.277)	(0.645)	(0.321)	(0.207)	(0.321)	(0.116)
Hansen J statistic	1.572	0.291	1.632	1.672	1.030	3.022
	(0.210)	(0.590)	(0.201)	(0.196)	(0.310)	(0.082)
Observations	4,160	4,160	4,160	4,160	4,160	4,160
Control	YES	YES	YES	YES	YES	YES
Year/Province	YES	YES	YES	YES	YES	YES

Notes: The P-value of Sargan-Hansen test is in parentheses; The Hansen J statistic applies a clustering-robust standard error criterion that accommodates clustering at the city level. In contrast, the Sargan-Hansen test and the Basmann test do not employ clustering robustness criteria in their evaluation of errors clustered at city level.

Table C3 provides an insightful analysis of underidentification and weak instrument tests for the instrumental variables *Ratio03* and *Ratio05*. The table showcases results from Kleibergen-Paap rk LM, Kleibergen-Paap rk Wald F, and Cragg-Donald Wald F tests. The Kleibergen-Paap rk LM test yields high statistics (ranging from 15.071 to 109.081) with significant P-values (all zero or close to zero), strongly suggesting that the model is well-identified and that the issue of underidentification does not exist for these instrument sets. Similarly, the Kleibergen-Paap rk Wald F test and the Cragg-Donald Wald F test exhibit high F statistics, well above these critical values, further confirming the strength of the instruments.

Table C3
Tests of underidentification and weak instrument for instrument variable (Ratio03 & Ratio05).

DV: *Carbon*	*Build-Carbon*			*City-Carbon*		
EV: *Shape*	(1) *Circle*	(2) *Cohesion*	(3) *Continuity*	(4) *Circle*	(5) *Cohesion*	(6) *Continuity*
Kleibergen-Paap rk LM	15.071	52.077	109.081	15.071	52.077	30.061
	(0.000)	(0.000)	(0.000)	(0.001)	(0.000)	(0.000)
Kleibergen-Paap rk Wald F	13.900	36.352	65.061	13.900	36.352	22.211
Cragg-Donald Wald F	22.978	77.193	88.309	22.978	77.193	20.976
Observations	4,160	4,160	4,160	4,160	4,160	4,160
Control	YES	YES	YES	YES	YES	YES
Year/Province	YES	YES	YES	YES	YES	YES

Notes: The P-value of Sargan-Hansen test is in parentheses; Stock-Yogo weak ID test critical values for 10% maximal IV size is 19.93, for 15% maximal IV size is 11.59, for 0% maximal IV size is 8.75, for 25% maximal IV size is 7.25.

As posited by DellaVigna and Kaplan (2007), the integrity of regression analyses is fortified by meticulously controlling for variables that may serve as possible pathways. In Table C4 and Table C5, the analysis focuses on the carbon emissions (*Build-Carbon* and *City-Carbon*) while controlling for population growth and the ratio of developable land across the entire administrative region for exclusivity test. Despite these controls, the "*Shape*" variable (which includes *Circle, Cohesion*, and *Continuity*) remains statistically significant across all specifications. This consistency suggests that the impact of urban form on carbon emissions is not confounded by direct effects of population growth or the broader ratio of developable land. The robustness of the "*Shape-b,*" "Kink_slope," and "Threshold value" coefficients under different control conditions reinforces the argument that our IVs exert their influence through the channel of urban form, rather than through direct impacts associated with population dynamics or extensive land development. These results from Tables C4 and C5 highlight the effectiveness of our IVs in isolating the impact of urban form on carbon emissions.

Table C4
Instrumental variables regression with additional controls (DV: *Build-Carbon*).

DV: *Build-Carbon*	Controlling Population Growth			Controlling of Full-scale Developable Land Ratio		
EV: *Shape*	(1) *Circle*	(2) *Cohesion*	(3) *Continuity*	(4) *Circle*	(5) *Cohesion*	(6) *Continuity*
Shape-b	-0.215***	-0.097***	-0.357***	-26.931***	-1.936***	-4.618***
	(-10.188)	(-6.713)	(-28.206)	(-18.314)	(-3.532)	(-9.302)
Kink_slope	0.273***	1.154***	1.140***	45.428***	21.140***	144.741***
	(18.747)	(24.012)	(11.856)	(28.773)	(8.298)	(15.763)
Threshold value	0.507***	0.751***	0.900***	0.543***	0.697***	0.960***
	(11.508)	(99.462)	(125.428)	(72.758)	(46.252)	(562.959)
Observations	3,900	3,900	3,900	3,900	3,900	3,900
Year	YES	YES	YES	YES	YES	YES
City	YES	YES	YES	YES	YES	YES

Table C5
Instrumental variables regression with additional controls (DV: *City-Carbon*).

DV: *City-Carbon*	Controlling Population Growth			Controlling of Full-scale Developable Land Ratio		
EV: *Shape*	(1) *Circle*	(2) *Cohesion*	(3) *Continuity*	(4) *Circle*	(5) *Cohesion*	(6) *Continuity*
Shape-b	-1.335***	-1.046***	-0.361***	-33.133***	-6.026***	-22.090***
	(-20.300)	(-16.902)	(-20.060)	(-17.087)	(-7.528)	(-33.409)
Kink_slope	1.893***	1.617***	2.235***	74.294***	40.526***	-73.662***
	(24.340)	(29.610)	(17.759)	(32.672)	(33.953)	(-5.063)
Threshold value	0.528***	0.451***	0.919***	0.598***	0.582***	0.961***
	(87.282)	(42.478)	(285.443)	(135.727)	(72.862)	(203.581)
Observations	3,900	3,900	3,900	3,900	3,900	3,900
Year	YES	YES	YES	YES	YES	YES
City	YES	YES	YES	YES	YES	YES

According to Acemoglu et al. (2001) and Meng et al. (2023), the exogeneity of instrumental variables was tested using alternative instruments. Our analysis integrates additional instrumental variables (namely "*River*"), which represents the geographical exogeneity of rivers within urban landscapes, and "*Railways*," reflecting the historical exogeneity of railway development as of 1933. Along with our primary instrument, "*Ratio05*," these variables facilitate a detailed examination of the influence of urban form on carbon emissions, delineated into "*Build-Carbon*" for emissions within built-up areas and "*City-Carbon*" for emissions across the entire urban expanse. The regression results depicted in Table C7 reveal that these additional instrumental variables are significantly associated with carbon emissions. Intriguingly, upon controlling for these novel variables, the significance of the coefficient for our initial instrumental variable, "*Ratio05*" diminishes in specific models. This outcome bolsters our hypothesis that, under the assumption of the complete exogeneity of the new instrumental variables, the significance of "*Ratio05*" is predominantly channeled through its linkage with these supplementary instruments rather than a direct relationship with carbon emissions. Consequently, this evidence substantiates the efficacy and exogeneity of "*Ratio05*" as an instrumental variable.

To verify the exogeneity of our instrumental variables, in Table C8, we implemented Sargan-Hansen and Basmann tests, further augmented by the Hansen J statistic for combinations of "*Ratio05 & River*" and "*Ratio05 & Railways.*" The outcomes of these overidentification tests lend credence to the validity of our instruments, thereby affirming their suitability in isolating the causal impact of urban form on carbon emissions.

Table C7
Regression results of additional instrumental variables for exclusivity test.

DV: *Carbon*	Less than threshold value		More than threshold value	
EV: *Circle*	(1) *Build-Carbon*	(2) *City-Carbon*	(3) *Build-Carbon*	(4) *City-Carbon*
Panel B: second stage regressions with *Ratio05* as an exogenous variable; IV: *River*				
Circle	-0.300*	-43.971***	0.941**	48.512**
	(-1.903)	(-3.276)	(2.248)	(2.374)
Ratio05	3.783	14.061	20.507	-5.307
	(0.907)	(1.514)	(1.246)	(-1.089)
UI test	15.05***	9.043***	7.764***	4.516**
WI test	9.991^	9.731^	3.663	4.733
Panel B: second stage regressions with *Ratio05* as an exogenous variable; IV: *Railways*				
Circle	-0.101*	-92.513*	0.467	47.095***
	(-1.758)	(-1.681)	(1.572)	(3.411)
Ratio05	0.005	19.117	5.811	-14.386
	(0.008)	(0.855)	(0.975)	(-1.542)
UI test	11.14***	9.448***	3.066*	6.168**
WI test	7.712	9.395^	3.025	6.634
Observations	889	607	2,871	3550
Year	YES	YES	YES	YES
Province	YES	YES	YES	YES

Note: The unidentifiable test (UI test) is the result of the Kleibergen–Paap rk LM statistic. The weak instrumental variable test (WI test) is the result of the Cragg–Donald Wald F statistic. ^, *, **, *** indicate significant at the significance level of 15%, 10%, 5%, and 1%, respectively.

Table C8
Tests of overidentification for additional instrument variable (*Ratio05& River / Railways*).

DV: *Carbon*	*Build-Carbon*		*City-Carbon*	
EV: *Circle*	(1) River	(2) Railways	(3) River	(4) Railways
Sargan-Hansen test	6.487	3.301	6.359	4.890
	(0.011)	(0.069)	(0.012)	(0.027)
Basmann test	6.416	3.262	6.290	4.835
	(0.011)	(0.071)	(0.012)	(0.028)
Hansen J statistic	6.579	14.756	7.118	14.756
	(0.010)	(0.000)	(0.008)	(0.000)
Observations	4,160	4,160	4,160	4,160
Control	YES	YES	YES	YES
Year/Province	YES	YES	YES	YES

Appendix D. Instrument variables one-stage regression results

Appendix D presents the robustness test results for substituting instrumental variables and the sample interval, taking the explanatory variable *Continuity* and *Cohesion* as an example. (iii) In Table D1 and Table D2 columns (1)-(2), we made a strategic switch in our approach by introducing the "*Ratio03*", which represents the proportion of developable land to the total land within a 300 m buffer, serving as the instrumental variable for urban form. (iv) To ensure a more robust testing process, in Table D1 and Table D2 columns (3)-(4), we've adjusted our approach by excluding data from the 2007–2008 period, which was marked by the financial crisis. (v) For a more comprehensive understanding, in Table D1 and Table D2 columns (5)-(6), we adjusted our dataset by excluding provincial capital cities. The outcomes align seamlessly with the primary conclusions presented earlier in the main content.

Table D1
Regression results of *Continuity* on carbon emissions (Replacing IV and sample).

DV: *Carbon*	Replacing IV		Replacing Time		Replacing Cities	
EV: *Continuity*	(1) *Build-Carbon*	(2) *City-Carbon*	(3) *Build-Carbon*	(4) *City-Carbon*	(5) *Build-Carbon*	(6) *City-Carbon*
Shape-b	-0.570***	-0.839***	-4.044***	-69.220***	-1.179***	-1.432***
	(-10.341)	(-38.008)	(-30.230)	(-11.336)	(-21.476)	(-19.621)
Kink_slope	0.764***	1.608***	3.997***	61.685***	2.152***	1.589***
	(16.445)	(28.018)	(29.702)	(10.532)	(44.486)	(25.616)
Threshold value	0.451***	0.486***	0.120***	0.109***	0.436***	0.236***
	(23.449)	(39.591)	(48.551)	(14.610)	(60.630)	(30.671)
Observations	4,160	4,160	3,640	3,640	3,776	3,776
Year	YES	YES	YES	YES	YES	YES
City	YES	YES	YES	YES	YES	YES

Table D2
Regression results of *Cohesion* on carbon emissions (Replacing IV and sample).

DV: *Carbon*	Replacing IV		Replacing Time		Replacing Cities	
EV: *Cohesion*	(1) *Build-Carbon*	(2) *City-Carbon*	(3) *Build-Carbon*	(4) *City-Carbon*	(5) *Build-Carbon*	(6) *City-Carbon*
Shape-b	-0.393***	-28.936***	-0.003	-10.265***	-0.303***	-24.921***
	(-24.583)	(-17.610)	(-0.457)	(-12.496)	(-8.254)	(-12.220)
Kink_slope	4.420***	85.373***	3.054***	24.252***	0.703***	51.452***
	(31.492)	(35.642)	(13.042)	(9.157)	(12.116)	(18.805)
Threshold value	0.924***	0.788***	0.948***	0.803***	0.775***	0.775***
	(461.198)	(98.210)	(358.828)	(55.422)	(28.973)	(39.889)
Observations	4,160	4,160	3,640	3,640	3,776	3,776
Year	YES	YES	YES	YES	YES	YES
City	YES	YES	YES	YES	YES	YES

References

Acemoglu, D., Johnson, S., Robinson, J.A., 2001. The colonial origins of comparative development: an empirical investigation. Am. Econ. Rev. 91, 1369–1401.
Angel, S., Chabaeva, A., Gitlin, L., Kraley, A., Parent, J.R., Perlin, M., 2005. Dyn. Glob. Urban Expans.
Angel, S., Franco, S.A., Liu, Y., Blei, A.M., 2020. The shape compactness of urban footprints. Prog. Plan. 139, 100429.
Baruah, N.G., Henderson, J.V., Peng, C., 2021. Colonial legacies: shaping African cities. J. Econ. Geogr. 21, 29–65.
Beaudry, C., Schiffauerova, A., 2009. Who's right, Marshall or Jacobs? The localization versus urbanization debate. Res Policy 38, 318–337.
Bettencourt, L., Lobo, J., Helbing, D., Kühnert, C., West, G., 2007. Growth, innovation, scaling, and the pace of life in cities. Proc. Natl. Acad. Sci. USA 104, 7301–7306.
Bibri, S.E., Krogstie, J., Kärrholm, M., 2020. Compact city planning and development: emerging practices and strategies for achieving the goals of sustainability. Dev. Built Environ. 4, 100021.

Boarnet, M.G., Hong, A., Santiago-Bartolomei, R., 2017. Urban spatial structure, employment subcenters, and freight travel. J. Transp. Geogr. 60, 267–276.
Boyko, C.T., Cooper, R., 2011. Clarifying and re-conceptualising density. Prog. Plan. 76, 1–61.
Cai, M., Ren, C., Shi, Y., Chen, G., Xie, J., Ng, E., 2023. Modeling spatiotemporal carbon emissions for two mega-urban regions in China using urban form and panel data analysis. Sci. Total Environ. 857, 159612.
Cai, M., Shi, Y., Ren, C., Yoshida, T., Yamagata, Y., Ding, C., Zhou, N., 2021. The need for urban form data in spatial modeling of urban carbon emissions in China: a critical review. J. Clean. Prod. 319, 128792.
Cervero, R., 1989. Jobs-housing balancing and regional mobility. J. Am. Plan. Assoc. 55, 136–150.
Cervero, R., Murakami, J., 2010. Effects of built environments on vehicle miles traveled: Evidence from 370 US Urbanized Areas. Environ. Plan. A 42, 400–418.
Chen, H., Jia, B., Lau, S.S.Y., 2008. Sustainable urban form for Chinese compact cities: challenges of a rapid urbanized economy. Habitat Int. 32, 28–40.
Chen, Z., Yu, B., Yang, C., Zhou, Y., Yao, S., Qian, X., Wang, C., Wu, B., Wu, J., 2021. An extended time series (2000–2018) of global NPP-VIIRS-like nighttime light data from a cross-sensor calibration. Earth Syst. Sci. Data 13, 889–906.
Chen, Z., Zhou, M., 2021. Urbanization and energy intensity: evidence from the institutional threshold effect. Environ. Sci. Pollut. R. 28, 11142–11157.
Cheng, L., Mi, Z., Sudmant, A., Coffman, D.M., 2022. Bigger cities better climate? Results from an analysis of urban areas in China. Energ. Econ. 107, 105872.
Cirilli, A., Veneri, P., 2014. Spatial structure and carbon dioxide (CO_2) emissions due to commuting: an analysis of italian urban areas. Reg. Stud. 48, 1993–2005.
Croci, E., Lucchitta, B., Janssens-Maenhout, G., Martelli, S., Molteni, T., 2017. Urban CO_2 mitigation strategies under the Covenant of Mayors: an assessment of 124 European cities. J. Clean. Prod. 169, 161–177.
Debbage, N., Shepherd, J.M., 2015. The urban heat island effect and city contiguity. Comput., Environ. Urban Syst. 54, 181–194.
DellaVigna, S., Kaplan, E., 2007. The fox news effect: media bias and voting. Q. J. Econ. 122, 1187–1234.
Dieleman, F., Wegener, M., 2004. Compact city and urban sprawl. Built Environ. (1978-) 30, 308–323.
Ding, G., Guo, J., Pueppke, S.G., Yi, J., Ou, M., Ou, W., Tao, Y., 2022. The influence of urban form compactness on CO_2 emissions and its threshold effect: evidence from cities in China. J. Environ. Manag. 322, 116032.
Duranton, G., Puga, D., 2000. Diversity and specialisation in cities: Why, where and when does it matter? Urban Stud. 37, 533–555.
Duranton, G., Puga, D., 2004. Chapter 48 - Micro-foundations of urban agglomeration economies. Handbook of Regional and Urban Economics. Elsevier, pp. 2063–2117.
Durst, N.J., 2021. Land use regulation and the spatial mismatch between housing and employment opportunities. Proc. Inst. Civ. Eng. - Urban Des. Plan. 174 (1), 15.
Ewing, R., Cervero, R., 2010a. Travel and the built environment. J. Am. Plan. Assoc. 76, 265–294.
Ewing, R., Cervero, R., 2010b. Travel and the built environment: a meta-analysis. J. Am. Plan. Assoc. 76, 265–294.
Falahatkar, S., Rezaei, F., 2020. Towards low carbon cities: spatio-temporal dynamics of urban form and carbon dioxide emissions. Remote Sens. Appl.: Soc. Environ. 18, 100317.
Fan, C., Tian, L., Zhou, L., Hou, D., Song, Y., Qiao, X., Li, J., 2018. Examining the impacts of urban form on air pollutant emissions: evidence from China. J. Environ. Manag. 212, 405–414.
Fang, C., Wang, S., Li, G., 2015. Changing urban forms and carbon dioxide emissions in China: a case study of 30 provincial capital cities. Appl. Energ. 158, 519–531.
Feng, Z., Peng, J., Wu, J., 2020. Using DMSP/OLS nighttime light data and K–means method to identify urban–rural fringe of megacities. Habitat Int. 103, 102227.
Frenken, K., Van Oort, F., Verburg, T., 2007. Related variety, unrelated variety and regional economic growth. Reg. Stud. 41, 685–697.
Gaigné, C., Riou, S., Thisse, J.-F., 2012. Are compact cities environmentally friendly? J. Urban Econ. 72, 123–136.
Gao, S., Zhang, X., Chen, M., 2022. Spatiotemporal dynamics and driving forces of city-level CO_2 emissions in China from 2000 to 2019. J. Clean. Prod. 377, 134358.
Gössling, S., Neger, C., Steiger, R., Bell, R., 2023. Weather, climate change, and transport: a review. Nat. Hazards 118, 1341–1360.
Hachaichi, M., Baouni, T., 2021. Virtual carbon emissions in the big cities of middle-income countries. Urban Clim. 40, 100986.
Hannah, L., Kay, J.A., 1977. The measurement of concentration. In: Hannah, L., Kay, J.A. (Eds.), Concentration in Modern Industry: Theory, measurement and the U. K. experience. Palgrave Macmillan UK, London, pp. 41–63.
Heinonen, J., Ottelin, J., Ala-Mantila, S., Wiedmann, T., Clarke, J., Junnila, S., 2020. Spatial consumption-based carbon footprint assessments - A review of recent developments in the field. J. Clean. Prod. 256, 120335.
Hong, S., Hui, E.C.-m, Lin, Y., 2022. Relationship between urban spatial structure and carbon emissions: A literature review. Ecol. Indic. 144, 109456.
Huang, Y., Yuquan, Z., 2019. Spatial spillover effect and driving forces of carbon emission intensity at the city level in China. J. Geogr. Sci. 29, 231–252.
IPCC, 2021. Climate change 2021: the physical science basis. Contribution of working group I to the sixth assessment report of the intergovernmental panel on climate change 2.
Jensen, P.D., 2016. The role of geospatial industrial diversity in the facilitation of regional industrial symbiosis. Resour. Conserv. Recycl. 107, 92–103.
Jim, C.Y., Chan, M.W.H., 2016. Urban greenspace delivery in Hong Kong: Spatial-institutional limitations and solutions. Urban For. Urban Green. 18, 65–85.
Jin, S., Nie, T., Pun, N., Xu, D., 2022. Spatial mismatch, different labor markets and precarious employment: The case of Hong Kong. Soc. Indic. Res. 161, 51–73.
Jiuwen, S., Xiaoxu, X., Qiangmin, X., Weihao, S., 2024. Impact of urban form on housing affordability stress in Chinese cities: Does public service efficiency matter? Cities 145, 104682.
Johnston, J., 1969. Economics and information theory (H. Theil). Econ. J. 79, 601–602.
Jung, M.C., Kang, M., Kim, S., 2022. Does polycentric development produce less transportation carbon emissions? Evidence from urban form identified by night-time lights across US metropolitan areas. Urban Clim. 44, 101223.
Kain, J.F., 1968. Housing segregation, negro employment, and metropolitan decentralization. Q. J. Econ. 82, 175–197.
Kennedy, C., Steinberger, J., Gasson, B., Hansen, Y., Hillman, T., Havranek, M., Pataki, D., Phdungsilp, A., Ramaswami, A., Mendez, G.V., 2010. Methodology for inventorying greenhouse gas emissions from global cities. Energ. Policy 38, 4828–4837.
Lan, T., Shao, G.F., Xu, Z.B., Tang, L.A., Dong, H.S., 2023. Considerable role of urban functional form in low-carbon city development. J. Clean. Prod. 392, 136256.
Li, Z., Wang, F., Kang, T., Wang, C., Chen, X., Miao, Z., Zhang, L., Ye, Y., Zhang, H., 2022a. Exploring differentiated impacts of socioeconomic factors and urban forms on city-level CO_2 emissions in China: Spatial heterogeneity and varying importance levels. Sustain. Cities Soc. 84, 104028.
Li, Z., Wu, H., Wu, F., 2022b. Impacts of urban forms and socioeconomic factors on CO_2 emissions: A spatial econometric analysis. J. Clean. Prod. 372, 133722.
Liu, F., Zhang, Z., Zhao, X., Liu, B., Wang, X., Yi, L., Zuo, L., Xu, J., Hu, S., Sun, F., Wang, Y., 2021a. Urban expansion of China from the 1970s to 2020 based on remote sensing technology. Chin. Geogr. Sci. 31, 765–781.
Liu, H., Huang, B., Zhan, Q., Gao, S., Li, R., Fan, Z., 2021b. The influence of urban form on surface urban heat island and its planning implications: Evidence from 1288 urban clusters in China. Sustain. Cities Soc. 71, 102987.
Liu, L., Tian, Y., 2022. Does the Compact City Paradigm Help Reduce Poverty? Evidence from China. Int. J. Environ. Res. Public Health 19, 6184.
Liu, X., Zhang, X., Sun, W., 2022a. Does the agglomeration of urban producer services promote carbon efficiency of manufacturing industry? Land Use Policy 120, 106264.
Liu, Y., Song, Y., Song, X., 2014. An empirical study on the relationship between urban compactness and CO_2 efficiency in China. Habitat Int. 41, 92–98.
Liu, Z., Deng, Z., He, G., Wang, H., Zhang, X., Lin, J., Qi, Y., Liang, X., 2022b. Challenges and opportunities for carbon neutrality in China. Nat. Rev. Earth Environ. 3, 141–155.
Liu, Z., He, C., Zhang, Q., Huang, Q., Yang, Y., 2012. Extracting the dynamics of urban expansion in China using DMSP-OLS nighttime light data from 1992 to 2008. Landsc. Urban Plan. 106, 62–72.
Luqman, M., Rayner, P.J., Gurney, K.R., 2023. On the impact of urbanisation on CO_2 emissions. npj Urban Sustain. 3, 6.
Mariaflavia, H., 2020. Cities in Bad Shape: Urban Geometry in India. Am. Econ. Rev. 110, 2377–2421.
Marshall, S., Gong, Y., Green, N., 2019. Urban compactness: New geometric interpretations and indicators. In: D'Acci, L. (Ed.), The Mathematics of Urban Morphology. Springer International Publishing, Cham, pp. 431–456.
Meng, L., Peng, L., Zhou, Y., 2023. Do housing booms reduce fertility intentions? Evidence from the new two-child policy in China. Reg. Sci. Urban Econ. 101, 103920.
Mia, P., Hazelton, J., James, G., 2019. Greenhouse gas emissions disclosure by cities: the expectation gap. Sustain. Account., Manag. Policy J. 10, 685–709.
Miguel, G.-A., Miriam, H.-R., Linna, L., 2016. The Causes of Urban Sprawl in Spanish Urban Areas: A Spatial Approach. Spat. Econ. Anal. 11, 219–247.
Ottelin, J., Ala-Mantila, S., Heinonen, J., Wiedmann, T., Clarke, J., Junnila, S., 2019. What can we learn from consumption-based carbon footprints at different spatial scales? Review of policy implications. Environ. Res. Lett. 14, 093001.
Ou, J., Liu, X., Wang, S., Xie, R., Li, X., 2019. Investigating the differentiated impacts of socioeconomic factors and urban forms on CO_2 emissions: empirical evidence from Chinese cities of different developmental levels. J. Clean. Prod. 226, 601–614.
Pichler, P.P., Zwickel, T., Chavez, A., Kretschmer, T., Seddon, J., Weisz, H., 2017. Reducing urban greenhouse gas footprints. Sci. Rep. 7, 14659.
Ramaswami, A., Jiang, D., Tong, K., Zhao, J., 2018. Impact of the economic structure of cities on urban scaling factors: implications for urban material and energy flows in China. J. Ind. Ecol. 22, 392–405.
Rao, Y., Dai, J., Dai, D., He, Q., 2021. Effect of urban growth pattern on land surface temperature in China: A multi-scale landscape analysis of 338 cities. Land Use Policy 103, 105314.
Santamouris, M., Cartalis, C., Synnefa, A., Kolokotsa, D., 2015. On the impact of urban heat island and global warming on the power demand and electricity consumption of buildings—A review. Energy Build. 98, 119–124.
Seo, M.H., Kim, S., Kim, Y.-J., 2019. Estimation of dynamic panel threshold model using Stata. Stata J. 19, 685–697.
Shannon, C.E., 1948. A mathematical theory of communication. Bell Syst. Tech. J. 27, 379–423.
Shi, F., Liao, X., Shen, L., Meng, C., Lai, Y., 2022. Exploring the spatiotemporal impacts of urban form on CO_2 emissions: Evidence and implications from 256 Chinese cities. Environ. Impact Assess. Rev. 96, 106850.
Shi, K., Xu, T., Li, Y., Chen, Z., Gong, W., Wu, J., Yu, B., 2020. Effects of urban forms on CO_2 emissions in China from a multi-perspective analysis. J. Environ. Manag. 262, 110300.
Simon, C.J., 1987. Industrial diversity, vacancy dispersion, and unemployment - [industrial diversity, industry structure, unemployment. Ann. Reg. Sci. 21, 60–73.
Su, Y., Chen, X., Li, Y., Liao, J., Ye, Y., Zhang, H., Huang, N., Kuang, Y., 2014. China's 19-year city-level carbon emissions of energy consumptions, driving forces and regionalized mitigation guidelines. Renew. Sustain. Energy Rev. 35, 231–243.

Sun, C.L., Zhang, Y.L., Ma, W.W., Wu, R., Wang, S.J., 2022. The impacts of urban form on carbon emissions: a comprehensive review. Land 11, 1430.
Van der Borght, R., Pallares Barbera, M., 2023. How urban spatial expansion influences CO_2 emissions in latin american countries. Cities 139, 104389.
Wang, D., Chai, Y., 2009. The jobs-housing relationship and commuting in Beijing, China: The legacy of Danwei. J. Transp. Geogr. 17, 30–38.
Wang, H., Lu, X., Deng, Y., Sun, Y., Nielsen, C.P., Liu, Y., Zhu, G., Bu, M., Bi, J., McElroy, M.B., 2019. China's CO_2 peak before 2030 implied from characteristics and growth of cities. Nat. Sustain. 2, 748–754.
Wang, S., Fang, C., Wang, Y., Huang, Y., Ma, H., 2015. Quantifying the relationship between urban development intensity and carbon dioxide emissions using a panel data analysis. Ecol. Indic. 49, 121–131.
Wang, S., Liu, X., Zhou, C., Hu, J., Ou, J., 2017. Examining the impacts of socioeconomic factors, urban form, and transportation networks on CO_2 emissions in China's megacities. Appl. Energ. 185, 189–200.
Wiedmann, T., Wood, R., Minx, J.C., Lenzen, M., Guan, D.B., Harris, R., 2010. A carbon footprint time series of the UK - Results from a multi-region input-output model. Econ. Syst. Res. 22, 19–42.
Wu, H., Fang, S., Zhang, C., Hu, S., Nan, D., Yang, Y., 2022. Exploring the impact of urban form on urban land use efficiency under low-carbon emission constraints: A case study in China's yellow river basin. J. Environ. Manag. 311, 114866.
Xia, C., Li, Y., Xu, T., Chen, Q., Ye, Y., Shi, Z., Liu, J., Ding, Q., Li, X., 2019. Analyzing spatial patterns of urban carbon metabolism and its response to change of urban size: A case of the Yangtze River Delta, China. Ecol. Indic. 104, 615–625.
Xia, L., Zhang, Y., Sun, X., Li, J., 2017. Analyzing the spatial pattern of carbon metabolism and its response to change of urban form. Ecol. Model. 355, 105–115.
Xiao, W., Li, H., Wei, Y.D., 2021. Understanding jobs-housing imbalance in urban China. A case study of Shanghai. J. Transp. Land Use 14, 389–415.
Yang, J., French, S., Holt, J., Zhang, X., 2012. Measuring the structure of U.S. metropolitan areas, 1970–2000. J. Am. Plan. Assoc. 78, 197–209.
Yang, S., Yang, X., Gao, X., Zhang, J., 2022. Spatial and temporal distribution characteristics of carbon emissions and their drivers in shrinking cities in China: Empirical evidence based on the NPP/VIIRS nighttime lighting index. J. Environ. Manag. 322, 116082.
Yang, Y., Ma, M., Zhu, X., Ge, W., 2020. Research on spatial characteristics of metropolis development using nighttime light data: NTL based spatial characteristics of Beijing. Plos One 15, e0242663.
Yu, Y., Sun, P., Xuan, Y., 2020. Do Constraints on Local Governments' Environmental Targets Affect Industrial Transformation and Upgrading. Econ. Res. J. 55, 57–72.
Zhang, Y., Zhang, S., Gong, Y., 2023. The Association between Carbon Emission and Urban Spatial Form—A Study of Zhuhai. China Land 12, 720.
Zhao, P., Lü, B., de Roo, G., 2010. Urban expansion and transportation: The impact of urban form on commuting patterns on the city fringe of Beijing. Environ. Plan. A: Econ. Space 42, 2467–2486.
Zhao, P., Lü, B., de Roo, G., 2011. Impact of the Jobs-housing Balance on Urban Commuting in Beijing in the Transformation Era. J. Transp. Geogr. 19, 59–69.
Zheng, S., Huang, Y., Sun, Y., 2022. Effects of Urban Form on Carbon Emissions in China: Implications for Low-Carbon Urban Planning. Land 11, 1343.
Zheng, Y., Cheng, L., Wang, Y., Wang, J., 2023. Exploring the impact of explicit and implicit urban form on carbon emissions: Evidence from Beijing, China. Ecol. Indic. 154, 110558.
Zhou, B., Rybski, D., Kropp, J.P., 2017. The role of city size and urban form in the surface urban heat island. Sci. Rep. 7, 4791.
Zhu, Y., Hu, Y., 2023. The Correlation between Urban Form and Carbon Emissions: A Bibliometric and Literature Review. Sustainability 15, 13439.
Zuiderwijk, A., Chen, Y.-C., Salem, F., 2021. Implications of the use of artificial intelligence in public governance: A systematic literature review and a research agenda. Gov. Inf. Q. 38, 101577.